

**FLOW THROUGH A PARTIALLY BLOCKED ARTERY DOWNSTREAM OF A
STENTED REGION**

A Thesis by

Aneesha Gogineni

Bachelors of Engineering, Jawaharlal Nehru Technological University, India 2009

Submitted to the Department of Mechanical Engineering
and the Faculty of the Graduate school of
Wichita State University
in partial fulfillment of
the requirements for the Degree of
Master of Science

July 2011

© Copyright 2011 by Aneesha Gogineni

All Rights Reserved

**FLOW THROUGH A PARTIALLY BLOCKED ARTERY DOWNSTREAM OF A
STENTED REGION**

The following Faculty members have examined the final copy of the Thesis for form and content and recommend that it be accepted in partial fulfillment of the requirement for the degree of Master of Science with a major in Mechanical Engineering.

T.S. Ravigururajan, Committee Chair

Ramazan Asmatulu, Committee Member

Lawrence Whitman, Committee Member

DEDICATION

*To my family, friends and my beloved god who gave me unconditional love and support
throughout this Thesis*

ACKNOWLEDGEMENTS

First of all I would like to thank my advisor Dr.T.S.Ravigururajan for his guidance and support throughout my masters at Wichita State University. I am particularly thankful to him for his patience while teaching me to write academic papers.

Besides my professor I would like to thank my committee members: Dr. Ramazan Asmatulu and Dr. Lawrence Whitman for taking time in reviewing my thesis. I also thank my friends Praneeth, Rohitha, Yaamunan, Harshi and Lavanya for their support in finishing my thesis.

Last but not least, I thank my parents and grandparents for their unconditional support and encouragement given to me in pursuing my interests. I would like to thank my god for being with me all the time.

ABSTRACT

A numerical analysis of flow through a stenosed artery downstream of a stented region is presented. Three different Food and Drug Administration (FDA) approved stents (Bx Velocity, NIR, and Multilink Zeta) are considered in analyzing pressure drop and flow rates at the blockage and outlet of artery. Blood flow inside the artery is assumed to be steady. The inlet pressures are defined as the mean arterial pressures in the stented artery using all stages of blood pressures. The pressure drop and volumetric flow rate increases at the blocked artery with increase in mean arterial pressures. In contrast to the previous results the pressure drop and volumetric flow rates decreases at the narrow end of the artery. A comparison was made between all the three different stents which determines the highly optimum stent geometry. An unsteady flow analysis is performed using NIR stent since it is proved to highly optimum when compared to other stents. The velocity and mass flow rates at the outlet are relatively high for unsteady flow rates when compared to steady flow rates. A grid independence study was also performed for all the three stents for accuracy. The obtained results can be used in determining the restenosis rates in patients after NIR stent implantation.

TABLE OF CONTENTS

Chapter	Page
1. INTRODUCTION	1
1.1 Motivation:.....	9
1.2 Objective:.....	10
2. LITERATURE REVIEW	11
3. METHODOLOGY	19
3.1 Method of Approach.....	19
3.2 Assumptions.....	20
4. APPLICATION	22
4.1 Pre and Post Processor.....	22
4.2 Governing Equations	23
4.3 Boundary Conditions	24
4.4 Computation Method	25
5. RESULTS AND DISCUSSION.....	28
5.1 Calculations and Observations.....	28
5.2 Grid Independence	53
6. CLINICAL SIGNIFICANCE.....	55
7. CONCLUSIONS AND FUTURE RECOMMENDATIONS.....	56
7.1 Conclusions.....	56
7.2 Future Recommendations	57
REFERENCES	59

LIST OF FIGURES

Figure	Page
1-1 Atherosclerolosis in artery.....	1
1-2 Balloon Inflation in blocked Artery.....	2
1-3 Stent Procedure before and after Surgery	3
1-4 Stent Insertion Procedure	4
1-5 Coronary Artery Disease	5
1-6 Blockage in Carotid Artery	6
1-7 Abdominal Aortic Aneurysm	7
1-8 Coronary Bypass Surgery	8
1-9 Stenosis in artery	9
3-1 Bx Velocity Stent.....	20
3-2 NIR Stent	20
3-3 Multilink Zeta Stent.....	21
4-1 Thirty percent Blocked Stented Artery.....	26
4-2 Fifty Percent Blocked Stented Artery.....	26
4-3 Seventy Percent Blocked Stented Artery.....	26
4-4 Eighty percent Blocked Stented Artery	26
4-5 2-D Model of Bx Velocity Stent.....	27
4-6 2-D Model of NIR Stent	27
4-7 2-D Model of Multilink Zeta Stent.....	27
5-1 Contours of Pressure for Thirty Percent Blockage.....	30

LIST OF FIGURES Contd...

Figure	Page
5-2 Contours of Pressure for Fifty Percent Blockage	30
5-3 Contours of Pressure for Seventy Percent Blockage	31
5-4 Contours of Pressure for Fifty Percent Blockage	31
5-5 Pressure Drop For Bx Velocity Stent	32
5-6 Volumetric Flow rate For Bx Velocity Stent.....	33
5-7 Pressure Drop For NIR Stent.....	35
5-8 Volumetric Flow rate For NIR Stent	36
5-9 Pressure Drop For Multilink Zeta Stent	37
5-10 Volumetric Flow rate For Multilink Zeta Stent.....	38
5-11 Pressure Drops for Thirty Percent Blockage	40
5-12 Pressure Drops for Fifty Percent Blockage	41
5-13 Pressure Drops for Seventy Percent Blockage	42
5-14 Pressure Drops for Eighty Percent Blockage	43
5-15 Contours of Unsteady Velocity for Thirty Percent Blockage.....	45
5-16 Contours of Unsteady Velocity for Fifty Percent Blockage.....	45
5-17 Contours of Unsteady Velocity for Seventy Percent Blockage.....	46
5-18 Contours of Unsteady Velocity for Eighty Percent Blockage.....	46
5-19 Unsteady Velocity Outlet at Thirty Percent Blocked Artery.....	47
5-20 Unsteady Velocity Outlet at Fifty Percent Blocked Artery.....	48
5-21 Unsteady Velocity Outlet at Seventy Percent Blocked Artery.....	49
5-22 Unsteady Velocity Outlet at Eighty Percent Blocked Artery.....	50

LIST OF FIGURES Contd...

Figure	Page
5-23 Velocity at Outlet of Artery.....	51
5-24 Mass Flow Rate at Outlet of artery.....	52
5-25 Grid Independence Check for Bx Velocity Stent	53
5-26 Grid Independence Check for NIR Stent.....	54
5-27 Grid Independence Check for Multilink Zeta Stent	54

NOMENCLATURE

μ ,	dynamic viscosity (Kg/m-s)
A	Amplitude during fluctuations (m/s)
A_1	Area of inlet region (m^2)
A_2	Area of outlet region (m^2)
g	gravity (m/s^2)
p,	pressure (Pa)
P_0	Initial pressure in the artery (Pa)
P_1	Pressure of inlet region (Pa)
P_2	Pressure of outlet region (Pa)
P_{avg}	Average pressure in the artery during cardiac cycle (Pa)
P_r	Pressure defined in the radial direction (Pa)
P_z	Pressure defined in the axial direction (Pa)
Q	Flow rate (m^3/s)
r	radius of the artery (m)
t	time that can be defined in post processor (s)
u_r ,	velocities defined in radial (m/s)
u_z	velocities defined in axial co-ordinates (m/s)
u_ϕ	velocities defined in tangential direction (m/s)
V_1	Velocity of inlet region (m/s)
V_2	Velocity of outlet region (m/s)
ρ	density (Kg/m ³) (Kg/m ³)
ω	Frequency at which heart beats(rad/s)

CHAPTER 1

INTRODUCTION

Atherosclerosis is a disease where plaque builds up inside arteries due to deposits of fatty substances, cholesterol, cellular waste products, calcium and other substances. Arteries carry oxygen rich blood to heart and other parts of the body, but over a period of time plaque limits the flow of oxygen rich blood. This leads to serious problems that include chest pain, shortness of breath, heart attack, stroke or even death. Sometimes pieces of plaque can break off and move through the affected artery to smaller blood vessels, followed by a blockage at artery causing tissue damage or sometimes even death. The best methods to treat advanced atherosclerosis include angioplasty, stenting, and coronary bypass surgery [1].

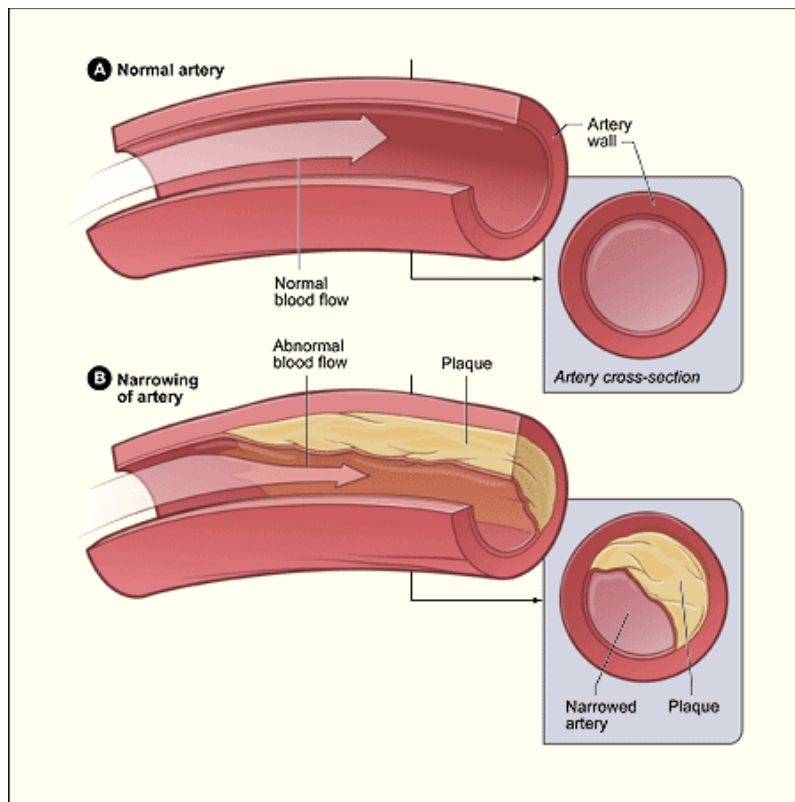


Figure 1-1 Atherosclerosis in artery[2]

Angioplasty:

An angioplasty is performed to reopen a partially blocked blood vessel to make the blood flow normal. Doctors use a special instrument as a means to see and take action inside arteries. As part of the test a catheter is introduced into an artery in the leg or arm. The catheter is gradually moved to the area where there is a blockage. By injecting a dye, blockages are seen through the visible x-ray screens and tiny tools are used at the catheter tip to open blockages. The risk of restenosis is highest in the first six months after angioplasty with rates as high as 35% [3].

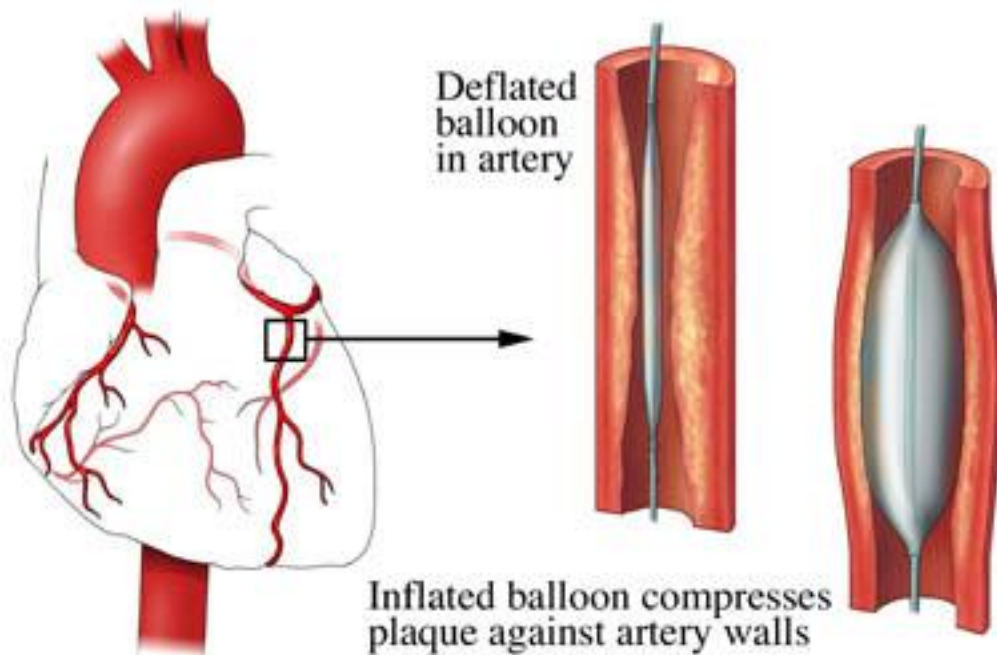


Figure 1-2 Balloon Inflation in blocked Artery[5]

Endovascular Stent Surgery:

In 1980, a surgical method was introduced to treat blockages in blood vessels which are caused by atherosclerosis. An endovascular stent placement will be recommended by a surgeon to treat atherosclerosis without using open surgery. Stent is a tiny cylinder of wire mesh used during an

angioplasty to open blocked segments of arteries. It is deployed through the catheter tip by inflating a balloon and this is done in conjunction with cleaning or repairing the artery. The process of enlarging the artery walls to improve the blood flow reduces the patients stay in hospital followed by a speedy recovery.

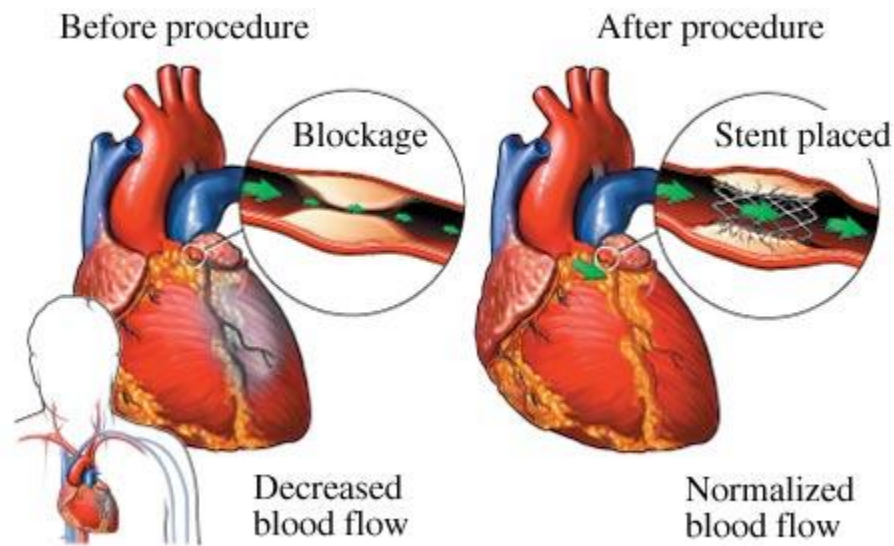


Figure 1-3 Stent Procedure before and after Surgery [6]

The stent surgery is performed in a cardiac catheterization laboratory with all the required equipment. A small portion of internal leg from the upper portion will be cured with an antiseptic solution to insert a catheter into the patient. During the surgery the surgeon can observe the entire procedure using a fluoroscope. Stent expands the artery walls after guiding the balloon catheter into the blocked area. Finally the balloon is deflated and taken out of the vessel and this entire procedure takes about an hour to 90minutes. Cells and tissues will grow above the stent and thus it becomes an enduring part of functioning artery [4].

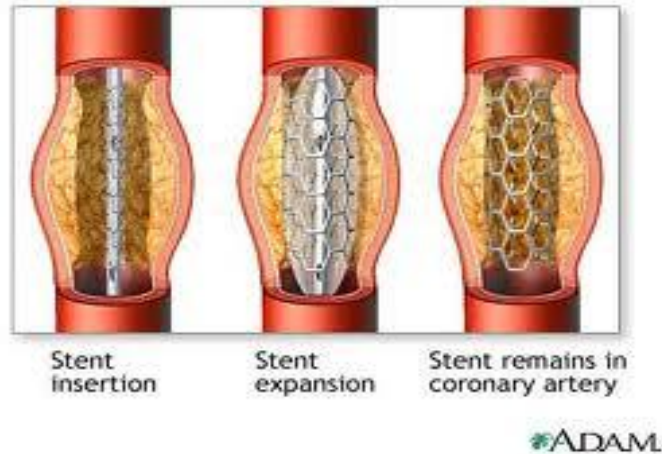


Figure 1-4 Stent Insertion Procedure [6]

Demographics:

In most of the other co-morbidities such as men and women suffer from heart disease and stroke. Additionally distinct food habits increases risks in many people. Every year stent surgeries are performed in more than seven lakh people to remove blockages in the coronary arteries. Also each year nearly 200,000 aortic aneurysms are diagnosed out of which 45000 people have surgery [4].

Circumstances Often Treated By Endovascular Stent Surgery:

- Coronary Artery Disease
- Narrowing of the Carotid Artery in Neck
- Aortic Aneurysm

Coronary Artery Disease is caused due to blockages in the arteries of the heart and these blockages are caused by fat deposits in the two main arteries which restricts the blood and

oxygen flow. These blockages might cause pain in the chest and in due course when there is an occlusion in the blood vessels, heart attack occurs in the patient.

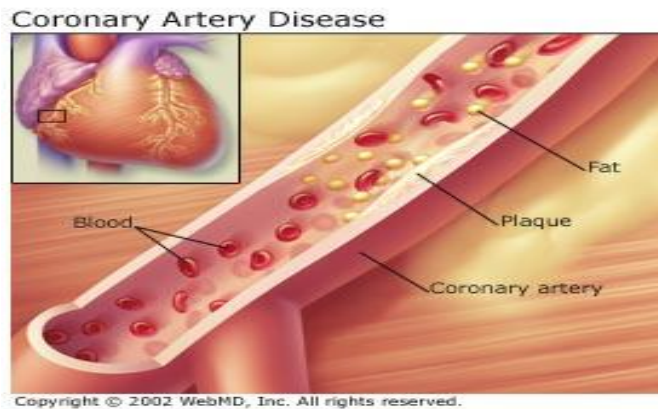


Figure 1-5 Coronary Artery Disease [7]

Carotid arteries in the neck

Due to gradual plaque formation in carotid arteries blood flow is interrupted causing a stroke. Apart from endovascular stent surgery, carotid endarterectomy surgery is another technique performed on people with significant stenosis. During the surgery fat material is removed in the arteries to allow a free flow of blood and oxygen. In spite of many advantages, this surgery causes high risks to patients. On the other hand, endovascular stent surgery is a less invasive procedure with fewer. The surgeon treating the patients helps them in preventing stroke during certain high risks.

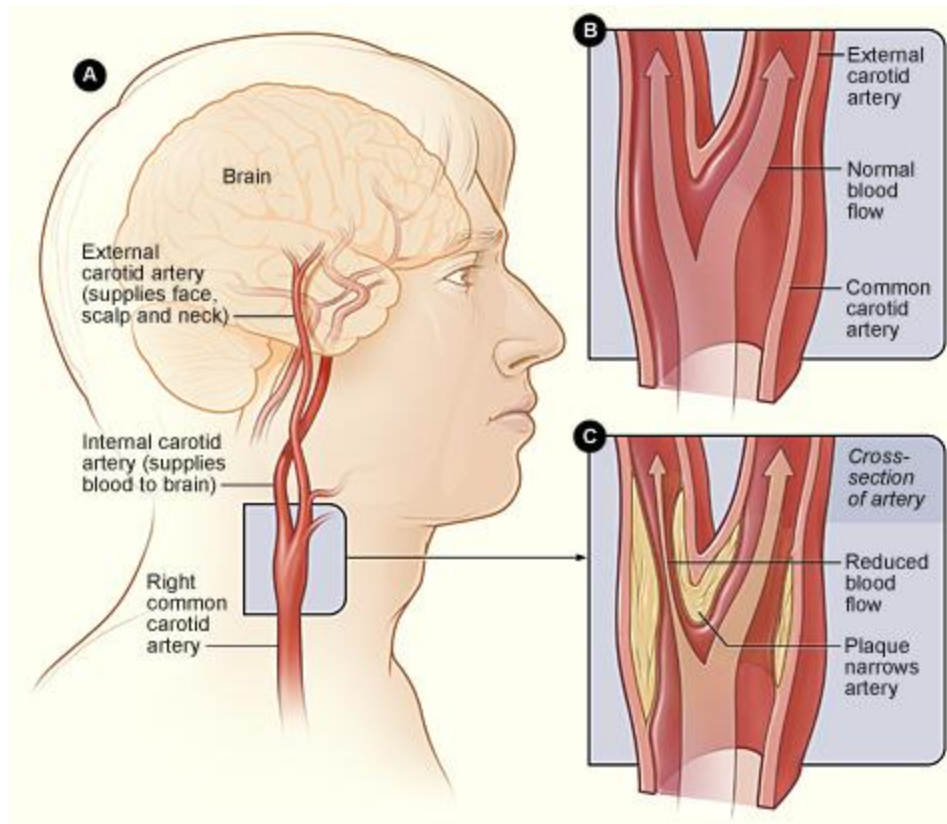


Figure 1-6 Blockage in Carotid Artery [8]

In Aortic aneurysm the pressure causes the area to swell along the major artery either in the abdomen or in the chest area. The aorta might ultimately undergo rupture causing immense bleeding and sometimes death. Aneurysms are sometimes diagnosed when the victim complains of pain, while in contrast to this sometimes there might not be any such symptoms also.

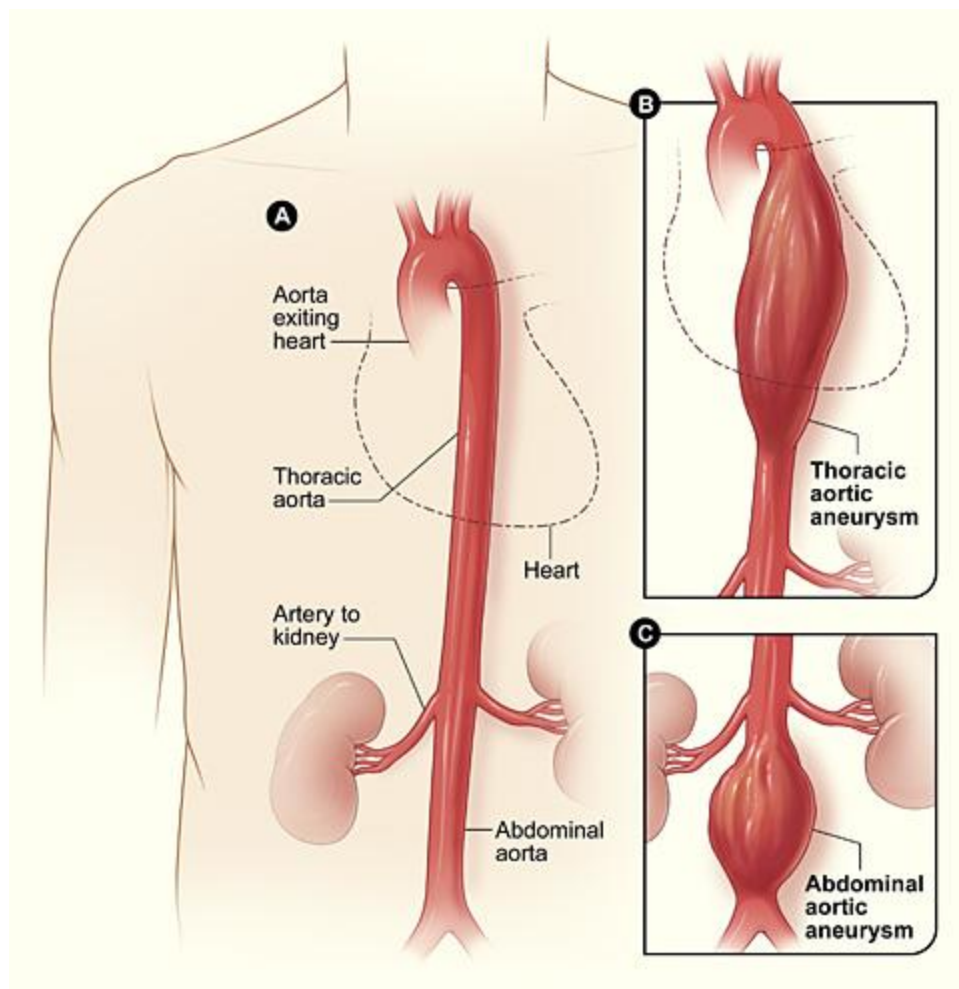


Figure 1-7 Abdominal Aortic Aneurysm [9]

Coronary bypass surgery:

A general anesthesia is administered prior to any activity and further a segment of the internal mammary artery is used for the graft which is taken from the leg, arm or chest. It is then sewed onto the clogged artery, rerouting blood around the clogged artery. Since this a major surgery, patients may experience complications like risk of bleeding, pneumonia or infection. Some other complications include graft closure or blockage, development of blockages in other arteries, damage to the aorta, high or low blood pressure, recurrence of angina and blood clots leading to stroke[4].

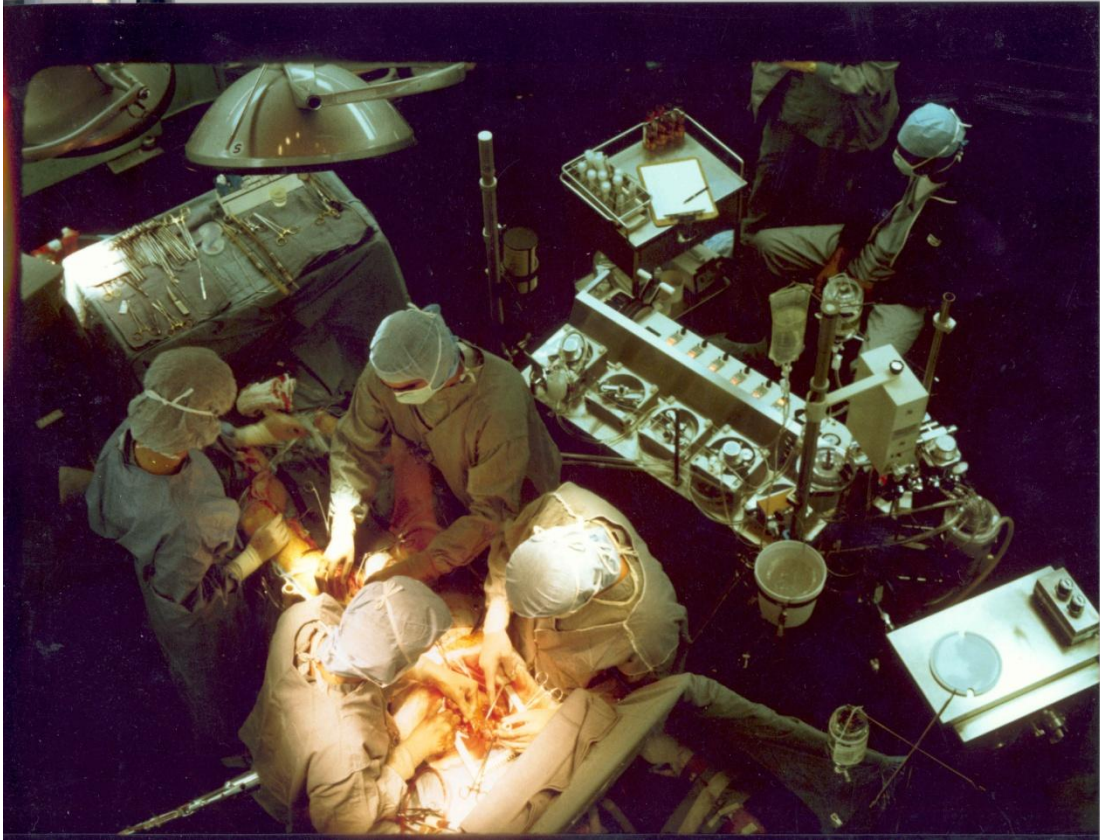


Figure 1-8 Coronary Bypass Surgery [10]

1.1 Motivation:

Multiple blockages:

Coronary artery disease can occur due to single blockage or multiple blockages and they can vary based on severity and location. These deposits narrow the coronary arteries which supplies less amounts of blood and oxygen to the heart. The decrease in blood flow causes chest pain, shortness of breath and sometimes heart attack.

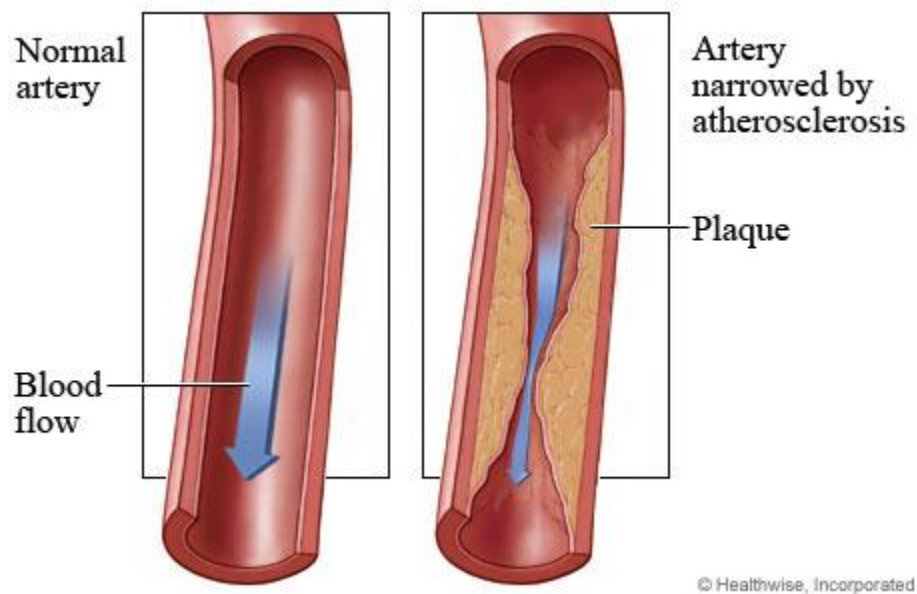


Figure 1-9 Stenosis in artery [11]

Stents cannot be placed in arteries at certain blockage levels because its structure do not fit in certain tapered and blocked arteries. In a multiple blocked artery stents are placed based on the level of possibility. So when one blockage is removed using stents the remaining blockages show effects of low blood and oxygen supply to the heart. These conditions have led to the computational fluid dynamic analysis of flow through partially blocked arteries downstream of stented region as current thesis.

1.2 Objectives:

The objectives of this study are to develop a computational methodology for simulating hemodynamic effect of in-stent restenosis in an artery with different blockages and to obtain a characterization of flow. Significant trials have shown the superiority of stenting over balloon angioplasty in terms of reduction of angiographic restenosis. Wide varieties of stents are used in the present days with different structural properties, design, material, composition and surface features. In addition, stents approved by FDA are preferred as they show low restenosis rates. However most of the results govern the stress field within the diseased lesions. Thus the correlation between stent designs, flow characteristics and pressure drops at blockages is not yet understood clearly. Hence the present analysis is developed to obtain flow characteristics, pressure drop and mass flow effects in blocked artery downstream of a stented region. Apart from this one other main objective is to determine an optimum stent design.

CHAPTER 2

LITERATURE REVIEW

Initially research was done on computational analysis of stent design and this was done to elucidate the mechanism of stenosis. Though stents have been successful in recent years, still they suffer from failure due to the formation of new tissue in stented segment. The author [13] made use of a two dimensional model and in the analysis a clear demonstration was given on strong dependence of flow stagnation on stent strut spacing. One other greatest difficulty was the neointimal growth over luminal aspect of stented artery which alters flow boundary geometry and thus these flow parameters were responsible for neointimal growth. Apart from flow stagnations there were few other parameters that account for increasing restenosis and that include wall shear stress.

From the test hypothesis, wall shear stress was altered in the computational fluid dynamic (CFD) analysis after coronary implantation of a stent. In order to construct the CFD models and evaluate wall shear stress at proximal and distal ends of the stented region, canine left anterior descending coronary artery blood flow velocity and diameter were used. Due to stent geometry there was a consequent channeling of adjacent blood layers that had a profound effect on wall shear stress. It was observed that stagnation zones were localized around stent struts. The results obtained depict alterations in wall shear stress caused by a stent and they support the theory of restenosis caused by stent geometry followed by a local wall shear stress distribution [14].

Besides wall shear stress, biomechanical interactions of stents and arteries were an important consideration for long term success. Restenosis was developed due to adverse arterial reaction to high stress. The author mainly focused on final arterial diameter and circumferential stress in

tapered arteries into which two different stents were placed. Finite Element Code was employed to solve the contact problem of artery wall made of strain stiffening material subjected to large deformation. That deformation rate includes 10% decrease in diameter over the length of the stent. A constant diameter and very high stresses at distal ends were obtained along the length of the stent when stiffer stent dominates over arterial taper. In contrast, a less stiff stent model follows close tapered contours which resulted in low artery wall stresses [15].

The three major factors that contribute to restenosis were (a) mechanical damage to the artery wall due to stent implantation (b) interaction between blood constituents and stent (c) oscillating wall shear stress caused by endothelial growth stimulation. Out of the three factors the last one was selected and a numerical model of restenosis was elaborated based on wall shear stress distribution in stented artery. Results for realistic geometric patterns of a progressing lumen reduction were obtained from the numerical simulation of in-stent restenosis. From the applied CFD analysis, regions subjected to low wall shear stress and the one that were prone to intimal proliferation were localized. This analysis was quite successful in predicting the sequence of shapes that might be recognized for consecutive stages of restenosis [16].

Similar to the previous analysis the author mainly focused on wall shear stress based on the stent geometry and deployment ratio. The experimental analysis called in-vivo adopts a stent to artery diameter ratio in order to reduce vascular damage during deployment. Since the wall shear stress distributions were not comprehensively evaluated computational analysis was chosen. The test hypothesis was conducted based on geometric properties and extent of expansion of a deployed stent which differentially influences wall shear stress using three dimensional CFD modeling. These theoretical results suggest that stent geometry minimizes stent to vessel area

and reduce strut number which exposes the vessel to shear stress that were implicated in neointimal hyperplasia [17].

Coupled with the previous conditions shear stress was considered as a key role of restenosis formation and it is sensitive to stent geometry. Different stents were considered with and without flow divider and the local flow alterations were created which led to the comparison of hemodynamic effects of stent design properties on restenosis. Computational fluid dynamic analysis was done to compute blood pressure and shear stress values in three different sites that include stented arterial segment, pre-stent and post-stent regions. From the analysis it was observed that wall shear stress between stent struts were sensitive to strut spacing, profile of strut, number of struts and curvature. While modeling, a slight increase in angle between two sides of stent strut will decrease the critical wall shear stress values of intrastrut area. With the application of flow divider, wall shear stress and pressure gradient increases in stented segment. With the application of flow divider wall shear stress increases and it influences the blood flow pattern in proximal of stented segment. To minimize the indices of fluid dynamics concerned in neointimal hyperplasia it is suggested to consider local flow patterns created by stent [18].

In addition to the previous analysis different stents were considered to study the alterations of phase shift between pressure and flow waveform. Along with this a comparison was made on the hemodynamic effects of stent design on restenosis in stented human artery. Different stents were responsible for alterations in phase shift between pressure and flow waveform and thus was further studied in three major regions using Mat lab. The results prove that variations in phase shift were sensitive to stent geometry that alters wall shear stress distribution leading to growth of intimal thickening in stented segment. Among the different stents, stent strut with elliptical geometry is more appropriate than those with hexagonal and rectangular geometry. Similar to the

previous case it was suggested to consider local flow patterns created by stent to minimize indices of fluid dynamics concerned in neointimal hyperplasia since size of phase shift increases with flow divider [19].

Hemodynamic factors and stent design parameters affect in-stent restenosis process and this was proved using three dimensional computational modeling. Spatial and temporal distribution of artery wall shear stresses was investigated when the stents expand with different designs and strut thickness. In all the stent models oscillatory wall shear stress was observed to be in common. Vessel wall surfaces and stent surfaces were compared to locate maximum wall shear stress on the stent surface area. Stent design with two different thickness values were investigated to obtain the hemodynamic effects. In extension, wall shear stress values were noted which showed a low wall shear stress region for thicker strut [20].

Restenosis varies with respect to stent strut after stent implantation and any alterations in flow patterns along with wall shear stress can modulate intimal hyperplasia. In order to compare flow characteristics, wall shear stresses were estimated in the near strut region of realistic stent designs. Three geometric parameters i.e axial strut pitch, strut amplitude and radius of curvature were considered during its employment in artery. At the stent strut, stagnation points were localized to show that point at large distal have low wall shear stresses. At minimum flow conditions the wall shear stress between struts was low when compared to high flow rates by 10-12% percentage. Mean transverse shear stress were 30-50% of mean axial shear stress at largest points. Existence of longitudinal connector was proved to be inefficient since restoration of wall shear stress in models without its presence was 11% larger than its existence. Thus it is hard to predict stent design at fluid mechanics environment in an artery. The sensitivity of flow characteristics with respect to strut configuration could be partially responsible for restenosis.

The spacing between strut points should be larger in order to restore disturbed flow according to fluid dynamics and it is advisable to have struts in the flow direction so that they reduce area of flow recirculation [21].

Not only ordinary stents but also there are other significant stents that reduce restenosis and thus various two dimensional and three dimensional stent analyses were performed. A uniform distribution of molecules in the vascular wall gives the efficiency of local drug delivery using polymer coated stent. To have minimal blood loss the distribution of molecules should be uniform radially and longitudinally. The main difference of this study from previous ones includes three dimensional modeling along with realistic pathologic vessel wall [22].

In summary stent geometry has been playing a key role in the restenosis formation at arterial segment. Apart from shear stress analysis, it is necessary to obtain flow characteristics and pressure drop conditions during stenosis and restenosis. While different stents exist in the present day, it is necessary to have a detailed study of stents to improve the efficiency of blood flow in stented arteries. Hence the further study included comparison between stent designs, advancements in stent models, material and their applications.

Different stent designs were considered to compare the stent artery interaction, effects of arterial injury, cellular proliferation neointimal formation and arterial dimensions. From the clinical experiments it was proved that all four stent designs (BX Velocity, Multilink, Nitinol and Palmaz-Schatz) had similar injury scores, cellular proliferation indexes and adventitial areas. But there is a twofold increase in neointimal area due to nitinol stents. The rate of arterial injury caused by nitinol stents was similar to balloon expandable stents due to the self expanding nature of nitinol stents. In nitinol stents, neointimal cell density was reduced which accounts for extracellular matrix expansion leading to larger neointima in nitinol stents [23].

Similarly a comparison was done between two stents (Tristar & Wallstent), but this is to improve the hemodynamics in cerebral aneurysm. Computational fluid dynamic analysis was performed using high porosity stents with varying vessel wall curvature in aneurysm models. The hemodynamic parameters such as aneurysm inlet flow, stasis and wall shear stress were investigated to observe related changes in specific designs. The parameters like stent porosity, strut design and a mesh hole shape were responsible for flow damping effect of stents, resulting aneurysm stasis and wall shear stress. It was also proved that flow damping effect of stent is considerably reduced at high vessel curvatures which indicate limited usefulness of high porosity stents. The flat mesh screen of stent has hydraulic resistance which predicts stasis - inducing performance of stents. Thus before running a full three dimensional simulation, cost effectiveness of three stent designs were compared [24].

Apart from strut design, stent porosity, stent artery interaction and so on, it is important to evaluate the properties and behavior of stents during stent expansion based on non-uniform balloon expansion. Along with this the mechanical characteristics should be determined since it improves the performances driven by it. Therefore seven commercial stents were considered in terms of Food and Drug Administration and they were analyzed based on Finite Element Analysis. The obtained results indicate that stents composed of opened unit cell connected by bend shaped link structures improves mechanical characteristics of stent. Similarly a control on the geometric and morphologic features of unit cell strut or link structure at the distal end of stent improves mechanical characteristics of stent. The study provides a better method at the realistic transient non-uniform balloon stent expansion. This was achieved by analyzing characteristics, behaviors and other parameters which help to improve the ability of vascular stent [25].

Although many studies have tried to identify the effects of stent geometry on hemodynamics, still coronary stents face the problem of in-stent restenosis. Five different coronary stent designs were considered from clinical practices and hemodynamic difference arise due to difference in design. A computational fluid dynamic analysis was performed with pulsatile blood flow to extract flow features like recirculation zones, velocity profiles, wall shear stress and oscillatory shear indices. From the analysis it was observed that vessel wall regions with low, reverse and oscillatory wall shear stress are more susceptible to restenosis. The work also investigates the difference in the flow that arises purely due to differences in stent-shape. The parameters that affect the hemodynamic performance were length of the connectors in the cross flow direction and their alignment with the main flow [26].

Similarly two different models have been developed using advanced computational fluid dynamics to assess the hemodynamic impact of coronary stent implantation. For the analysis one model represents left anterior descending (LAD) coronary artery implanted with a Palmz-Schatz(PS) stent and the second model represents the same artery with Gianturco-Roubin-II (GR-II) stent. In order to simulate fully developed non-Newtonian nature of coronary blood flow, mathematical models were constructed. The characteristics responsible for restenosis were identified from computational analysis and it was observed to be low wall shear stress and high wall shear stress. The data obtained from clinical restenosis trials of GR-II and PS stent helps in investigating the correlations between flow characteristics and restenosis rates [27].

In spite of much analysis on various stent modeling it is also important to develop new models. Two different approaches (structural mechanism and finite element method) were chosen to survey basic properties of stents and list the basic designs. Apart from a lot of restrictions both approaches have effective application region. In order to optimize the delivery

diameter in relation to desired stiffness for a wire-woven spiral stent, analytical model is chosen as a flexible tool. But it is not advisable to apply it to more complicated shapes than spiral and from the study the model does not consider spiral as interwoven [28].

In addition to analysis of stent designs in coronary arteries, it is important to analyze aortic valve stent designs. Finite Element Analysis was done on four different percutaneous aortic valve stents using three biomaterials with different load range. The pressures involved in the analysis were selected based on the human blood pressure. These pressure and load selections were selected to understand the mechanical behavior of different stent designs under these conditions. The analysis on four different stents helped in generating physical, mechanical and behavioral properties of these stents. This also aided in understanding stents performance ranges when subjected to the pressures exerted by heart and cardiac blood flow during various cardiovascular conditions. Thus proper stent designs and biomaterials can be chosen under various circumstances of blood flows [29].

Hence the studies on comparing various stents show that it is necessary to find an appropriate stent design under several cardiovascular conditions. Thus, as part of my work three FDA approved stents were considered to give the best stent design.

CHAPTER 3

METHODOLOGY

3.1 Method of Approach

Initially a multiple blocked artery is considered in which the first blockage is replaced with a stent. Thus a two dimensional stented artery is modeled with different blockage rates at particular distance from the stent and consequently the artery gets narrowed. Three most commonly used FDA stents (Bx Velocity Stent, NIR Stent and Multilink Zeta Stent) are modeled in GAMBIT. Coupled with these conditions, all the three stents are modeled with different blockage levels. The required geometry is assumed which are further explained in detail. A steady blood flow analysis is done using FLUENT software in all the three stents at different blockages. Boundary conditions at the inlet and outlet are defined using different blood pressure levels that generally exist in humans. Comparisons of three stents are done based on the pressure drop values obtained at the blockage. Furthermore volumetric flow rates for all the different stents are obtained at different blockages. As an extension to the previous analysis a pulsatile blood flow is analyzed in optimum stented artery with different blockage rates. Based on the different inlet and outlet conditions of pressure, velocity and mass flow rates are obtained at the tapered end of the artery. To estimate the error, grid independence test is conducted for all the three stents by comparing course grid solution against those of finest grid.

3.2 Assumptions

Length of the artery=225mm

Diameter of the artery=3mm

Length of the Stent=11mm

Diameter of the artery=3mm

Tapered length of the artery from stent to blockage=120mm

Length of the blockage=5mm

Diameter of the artery at the blockage=2mm

Length of the artery from blockage to the assumed end of artery=75mm

Diameter of the artery at the assumed tapered end =1mm

Stent Struts in Three Dimensional View

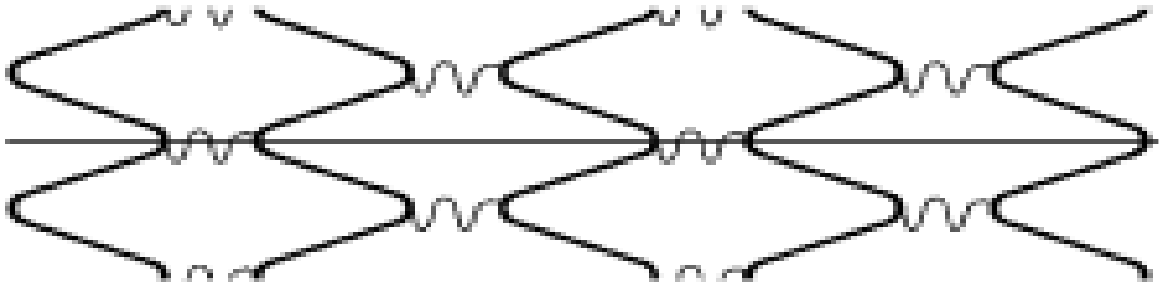


Figure 3-1 Bx Velocity Stent



Figure 3-2 NIR Stent

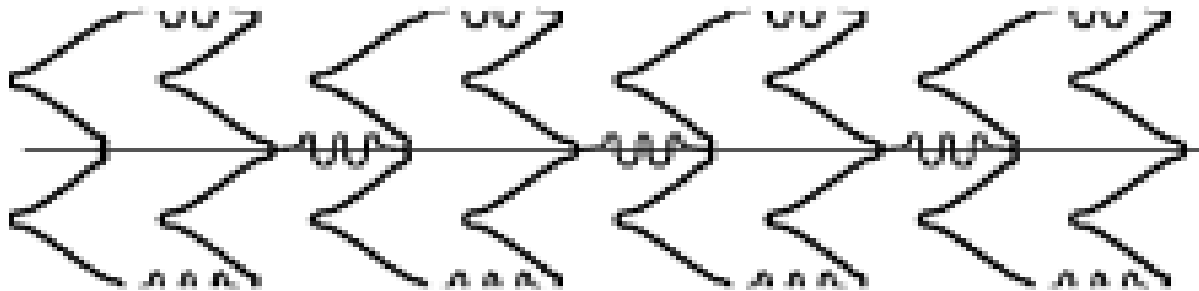


Figure 3-3 Multilink Zeta Stent

CHAPTER 4

APPLICATION

4.1 Pre and Post Processor

Prior to the analysis a two dimensional model was developed using GAMBIT (version 2.4.6) software. The special points were defined on the stent area and they are connected to each other along with necessary wires. The profile for stent strut was joined according to the assumed geometry and the blockage in artery was modeled consecutively. The stent was supposed to be in a vessel with same diameter and thus the combination of vessel and stent is like a vessel that a stent was implanted on it. The flow region for normal and stented vessels were discretized with T-grid algorithm of commercial software GAMBIT. It is necessary to specify face mesh in GAMBIT; however the vertex types associated with its faces along with shape and topology determines the mesh density.

Post Processor

The commercial software FLUENT (version 12) was applied to solve the the governing equations. It provides comprehensive advanced modeling potentials for a wide range of laminar, turbulent, incompressible and compressible fluid flow problems. Besides this fluent has the ability to model complex geometries along with a broad range of mathematical models for transport phenomenon. The governing equations and boundary conditions needed for the analysis were mentioned in detail in the next chapters. As soon as the model is imported from the pre-processor the mesh density is checked for accuracy. The default units were modified so that all the dimensions and obtained results will be in the same units.

4.2 Governing Equations

The flow inside an artery is considered to be incompressible and blood is a Newtonian fluid with constant fluid properties. The continuity and Navier-stokes equation for a two dimensional cylindrical co-ordinates (r,z) can be written in differential conservation form which is shown below.

Continuity Equation for three dimensional axes (r,φ,z):

$$r: \rho(\partial u_r / \partial t + u_r \partial u_r / \partial r + (u_\phi / r) \partial u_r / \partial \Phi + u_z \partial u_r / \partial z - u_\phi^2 / r) = -\partial p / \partial r + \mu[(1/r) \partial / \partial r (r \partial u_r / \partial r) + 1/r^2 \partial^2 u_r / \partial \Phi^2 + \partial^2 u_r / \partial z^2 - u_r / r^2 - 2/r^2 \partial u_\phi / \partial \Phi] + \rho g_r$$

$$\Phi: \rho(\partial u_\phi / \partial t + u_r \partial u_\phi / \partial r + (u_\phi / r) \partial u_\phi / \partial \Phi + u_z \partial u_\phi / \partial z + u_r u_\phi / r) = -1/r \partial p / \partial \Phi + \mu[(1/r) \partial / \partial r (r \partial u_\phi / \partial r) + 1/r^2 \partial^2 u_\phi / \partial \Phi^2 + \partial^2 u_\phi / \partial z^2 + 2/r^2 \partial u_r / \partial \Phi - u_\phi / r^2] + \rho g_\phi$$

$$z: \rho(\partial u_z / \partial t + u_r \partial u_z / \partial r + (u_\phi / r) \partial u_z / \partial \Phi + u_z \partial u_z / \partial z) = -\partial p / \partial z + \mu[(1/r) \partial / \partial r (r \partial u_z / \partial r) + 1/r^2 \partial^2 u_z / \partial \Phi^2 + \partial^2 u_z / \partial z^2] + \rho g_z$$

For two dimensional axes (r,z)

$$(1/r * \partial(r u_r) / \partial r) + \partial u_z / \partial z = 0$$

For axisymmetric flow there is no tangential velocity ($u_\phi=0$) and gravity effects were neglected.

r-directional momentum equation:

$$\partial u_r / \partial t + u_r \partial u_r / \partial r + u_z \partial u_r / \partial z = -1/\rho \partial p / \partial r + \mu/\rho [\partial / \partial r (1/r \partial(r u_r) / \partial r) + \partial^2 u_r / \partial z^2]$$

Z-direction momentum equation:

$$\partial u_z / \partial t + u_r \partial u_z / \partial r + u_z \partial u_z / \partial z = -1/\rho \partial p / \partial z + \mu/\rho [1/r \partial / \partial r (r \partial u_z / \partial r) + \partial^2 u_z / \partial z^2]$$

4.3 Boundary Conditions

The boundary conditions used in the present computation are

Steady flow Condition:

At inlet:

$$\partial p_r / \partial z = \text{Constant},$$

At the outlet:

$$\partial p_r / \partial z = \partial p_z / \partial z = 0$$

At the wall:

$$\text{No slip flow condition: } u_z=0$$

For Unsteady Flow Condition:

A periodic velocity boundary condition can be applied to the inlet of the tube using User Defined Function (UDF). The general equation from FLUENT user define Manual is as follows,

$$P_z=P_0+A\sin\omega t \text{ [31]}$$

At the inlet:

$$P_z=P_0+P_{\text{avg}}\sin\omega t$$

At the outlet:

$$\partial p_r / \partial z = \partial p_z / \partial z = 0$$

At the wall:

$$\text{No slip flow condition: } u_z=0$$

4.4 Computation Method

A two dimensional artery is modeled with four different blockage levels (30%, 50%,70% and 80%) at specific distance from stent, followed by a narrow region at the end of an artery using a pre-processor (Figure.4.1-4.4). The domain is subdivided into elements and the type of element selected for meshing the face of the model is triangular with an interval size of 0.2. Specific boundary conditions like the pressure inlet, pressure outlet and wall boundaries can be defined during pre-processor modeling and the continuum type of the model is selected as fluid. In addition to this three different stents are modeled to determine an optimum stent design in a multiple blocked artery, where one of the blockages is replaced with a stent (Figure.4.5-4.7). For further analysis this model is exported to post processor and mesh is checked for accuracy. To define the units scaling is done based on the geometry. If the analysis is in steady state pressure-based steady state solver is selected and for unsteady, pressure-based transient solver is selected. Blood is considered as a non-Newtonian fluid flowing through the artery with a density of 1050kg/m^3 and viscosity of $3.5\text{e}^{-3}\text{kg/m-s}$. The cell zone inside the artery is selected as blood and the boundary conditions can be defined based on steady and unsteady state. For an unsteady blood flow a user defined function is interpreted through a C-program and along with this surface monitors are selected based on the required field variable for every time step.

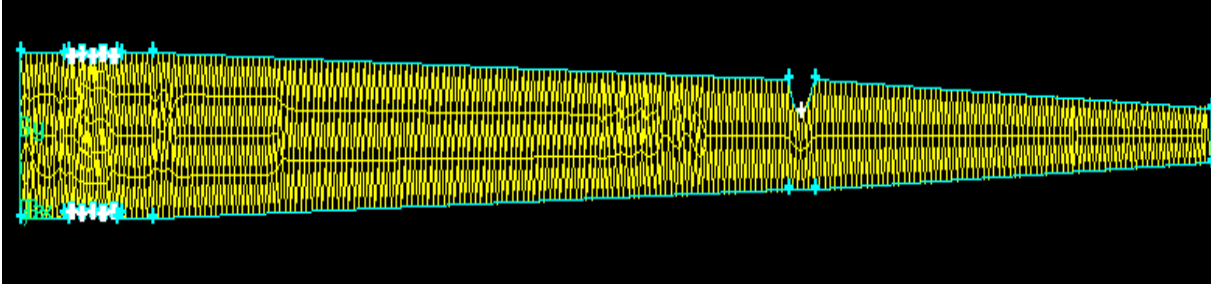


Figure 4-1 Thirty percent Blocked Stented Artery



Figure 4-2 Fifty Percent Blocked Stented Artery

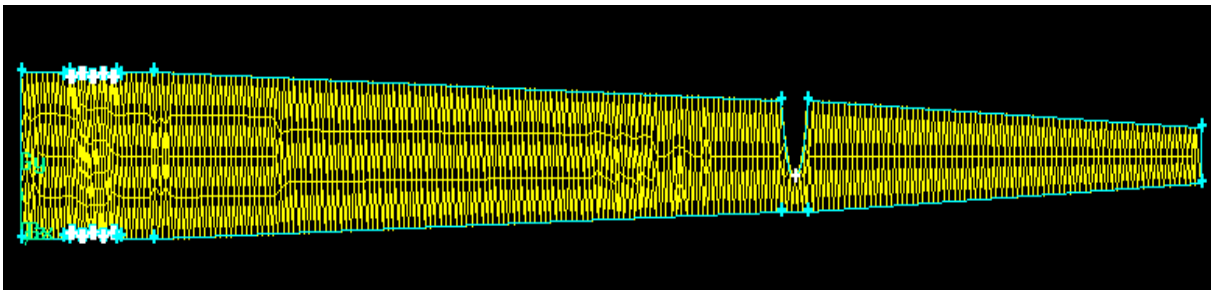


Figure 4-3 Seventy Percent Blocked Stented Artery

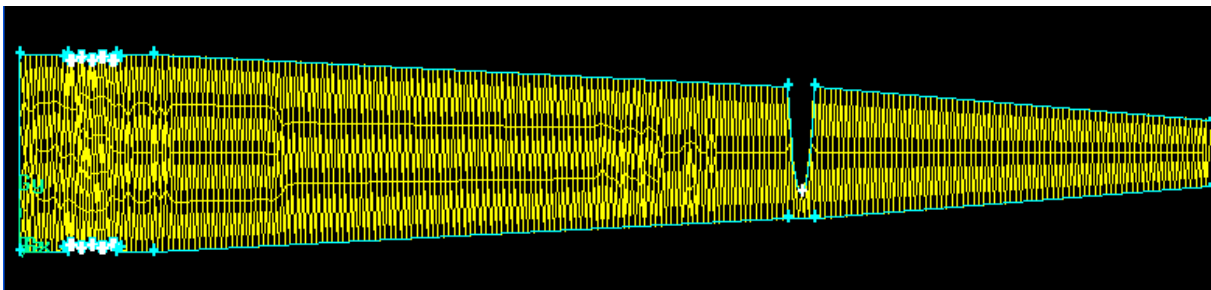


Figure 4-4 Eighty percent Blocked Stented Artery

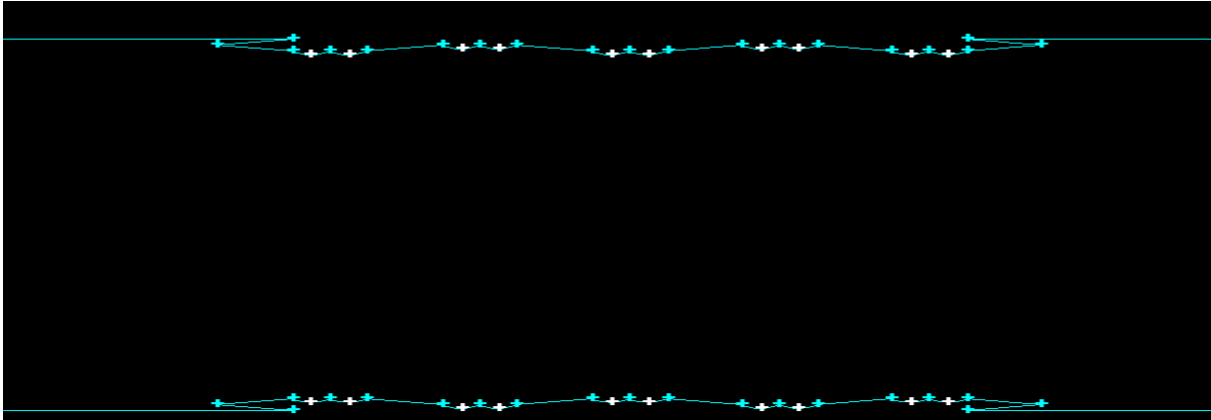


Figure 4-5 2-D Model of Bx Velocity Stent

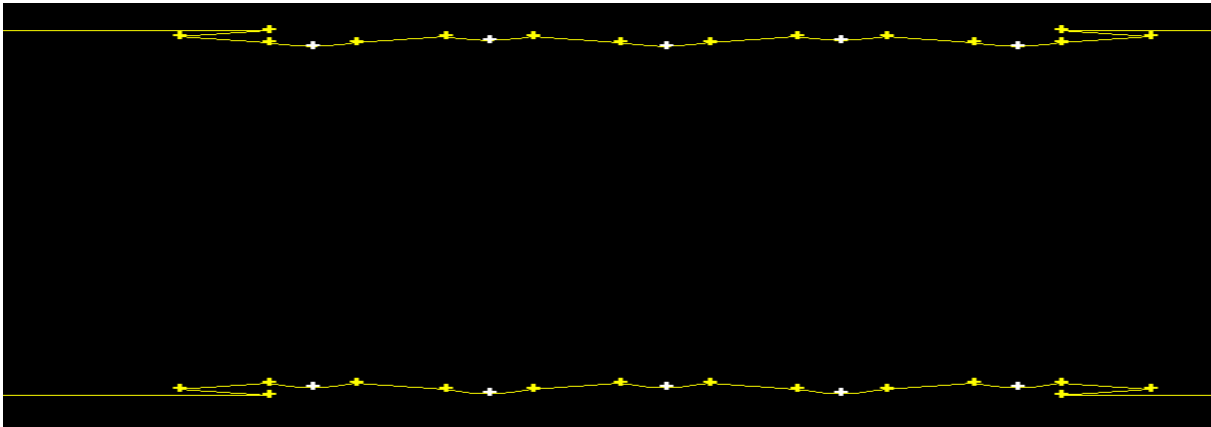


Figure 4-6 2-D Model of NIR Stent

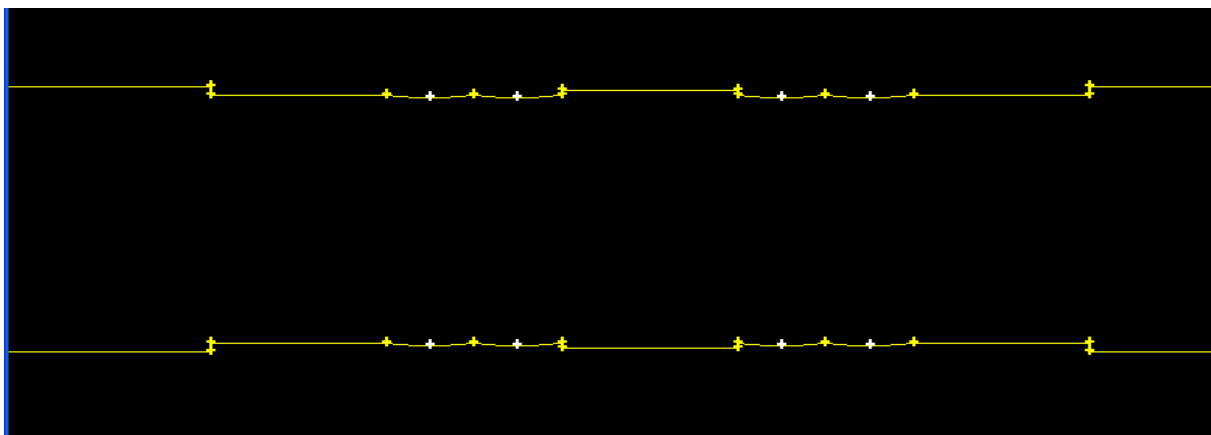


Figure 4-7 2-D Model of Multilink Zeta Stent

CHAPTER 5

RESULTS AND DISCUSSION

5.1 Calculations and Observations

Initially a steady state mean arterial pressure inlet boundary condition is defined to obtain the pressure at different blockage rates. Mean arterial pressure is defined as the average arterial pressure during single cardiac cycle. It can be determined from the measurements of systolic and diastolic pressures at various heart rates [33].

$$MAP=P_{dias}+1/3(P_{sys}-P_{dias})$$

Mean arterial pressure varies with respect to the blood pressure rates which are shown below[35]

Normal Blood Pressure-120-80mm of hg

Pre-Hypertension-130-85mm of hg

High blood pressure stage1-140-95mm of hg

High blood pressure stage1-150-105mm of hg

High blood pressure stage2-160-115mm of hg

Figure 5-1 below indicates the contours of pressure in a stented artery with multiple blockages. At the stenosed region the pressure decreases with an increase in percentage of stenosis thereby increasing the pressure drop at the highly restenosed artery. At outlet the pressure increases with increase in stenosis for thirty, fifty and seventy percent blockages (Figure.5-1 to 5-3). But the results are different in case of eighty percent blockage since the drop in pressure at stenosed region is high when compared to outlet due to the geometry variations at outlet and blockage.

From the mean arterial pressure inlets the pressure at the blockages are obtained for all the blockage rates of BX Velocity stent and it is observed that the pressure drop is high for eighty percent blockage since velocity at that region will be high (Figure.5-5).

As an extension to the previous obtained data, volumetric flow rate of stented artery with restenosis is noted using the standard continuity equation for incompressible flow in terms of pressure.

From the continuity equation [34]:

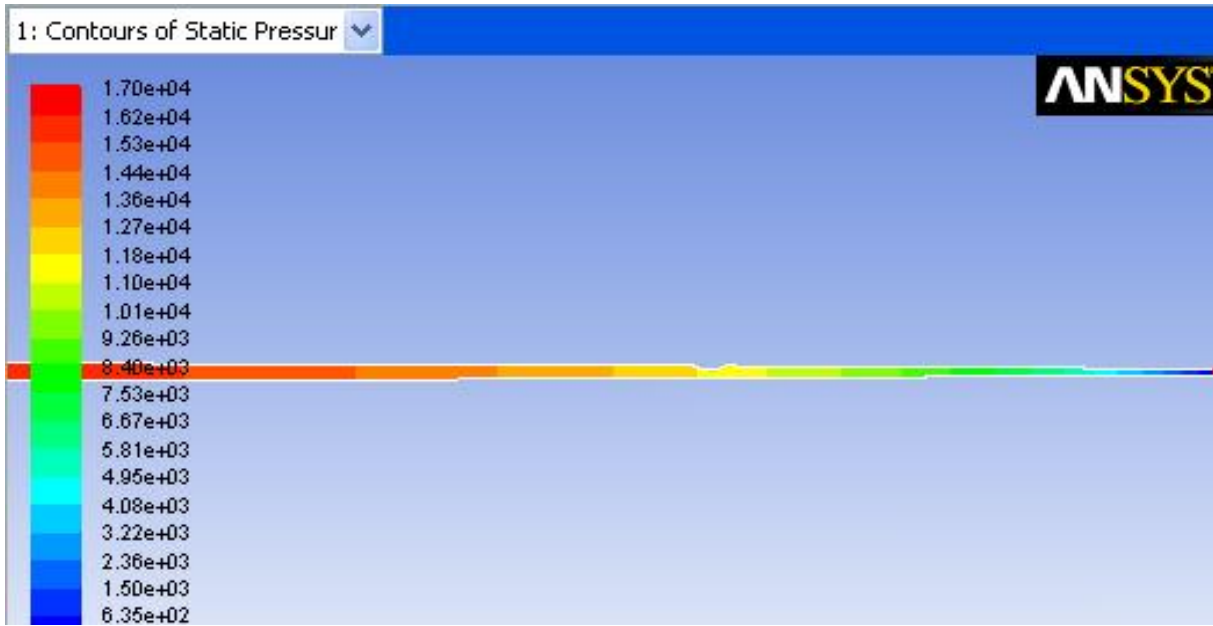
$$Q=A_1.V_1=A_2.V_2 \text{ or } V_1=Q/A_1 \text{ and } V_2=Q/A_2$$

$$P_1-P_2=1/2\rho(Q/A_2)^2-1/2 \rho(Q/A_1)^2$$

Equation is written in terms of pressure to obtain Q

$$Q=A_2[2(P_1-P_2)/\rho/1-(A_2/A_1)^2]^{1/2}$$

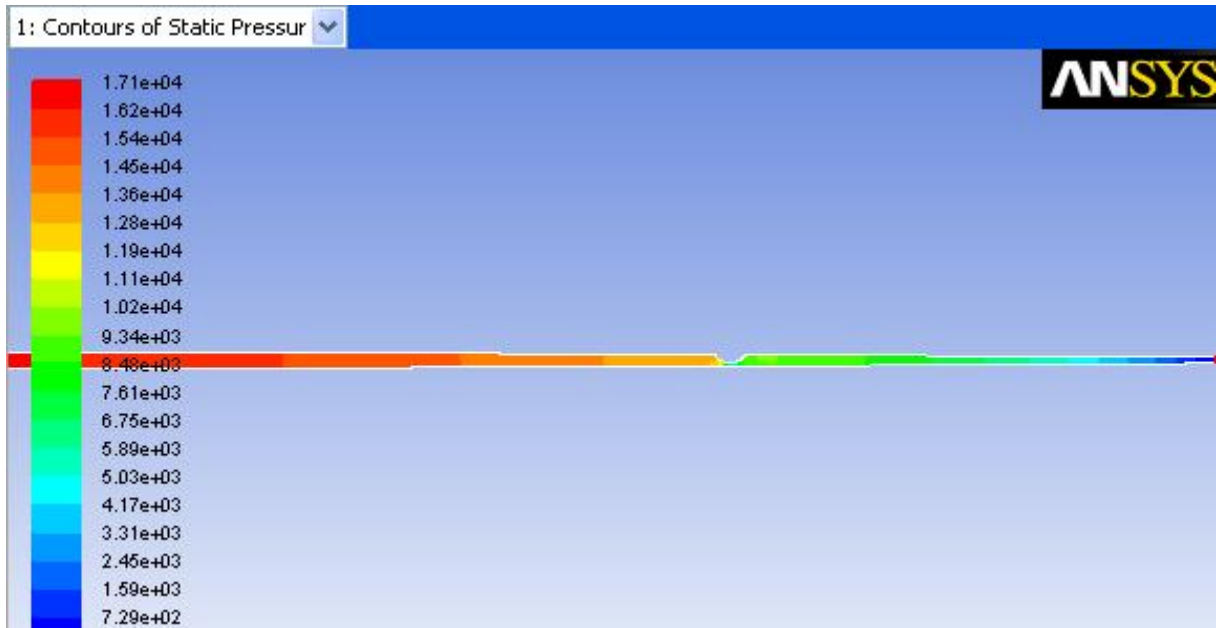
According to the results obtained, volumetric flow rate is also highest for a highly stenosed region when compared to the lower ones. Since flow rate is based on pressure drop, the obtained results were similar to the pressure drop at blockage. In addition to this the narrowed artery region next to the stenosed portion of Bx velocity stent showed that the volumetric flow rate is highest for a low stenosed region (Figure.5-6).



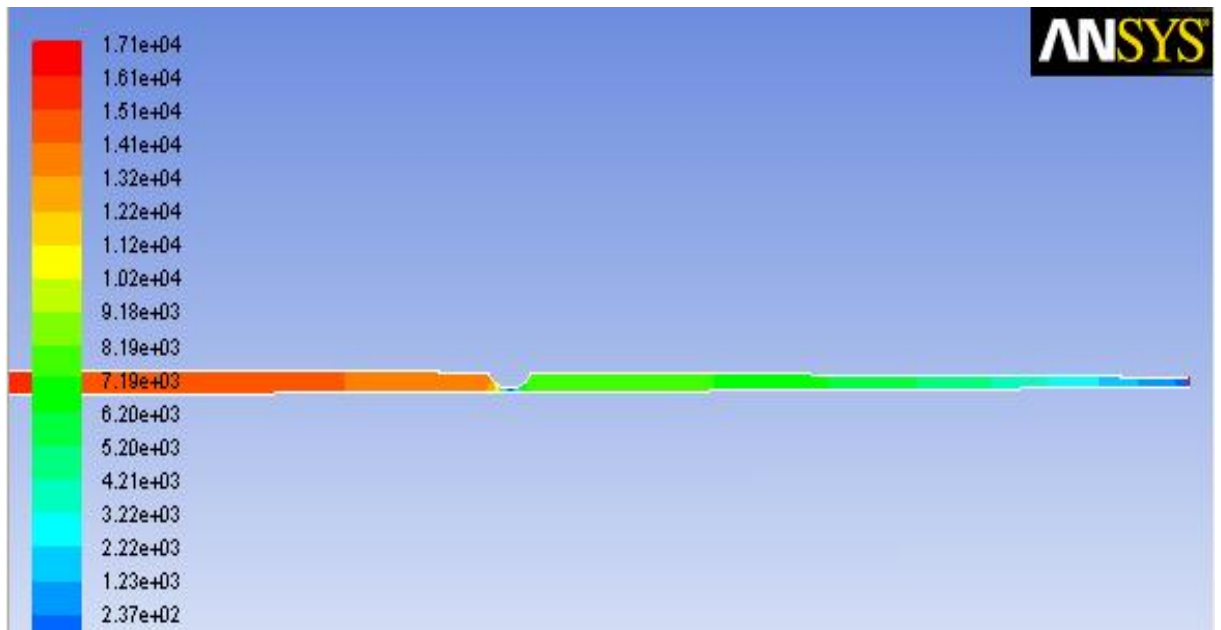
5-1 Contours of Pressure for Thirty Percent Blockage



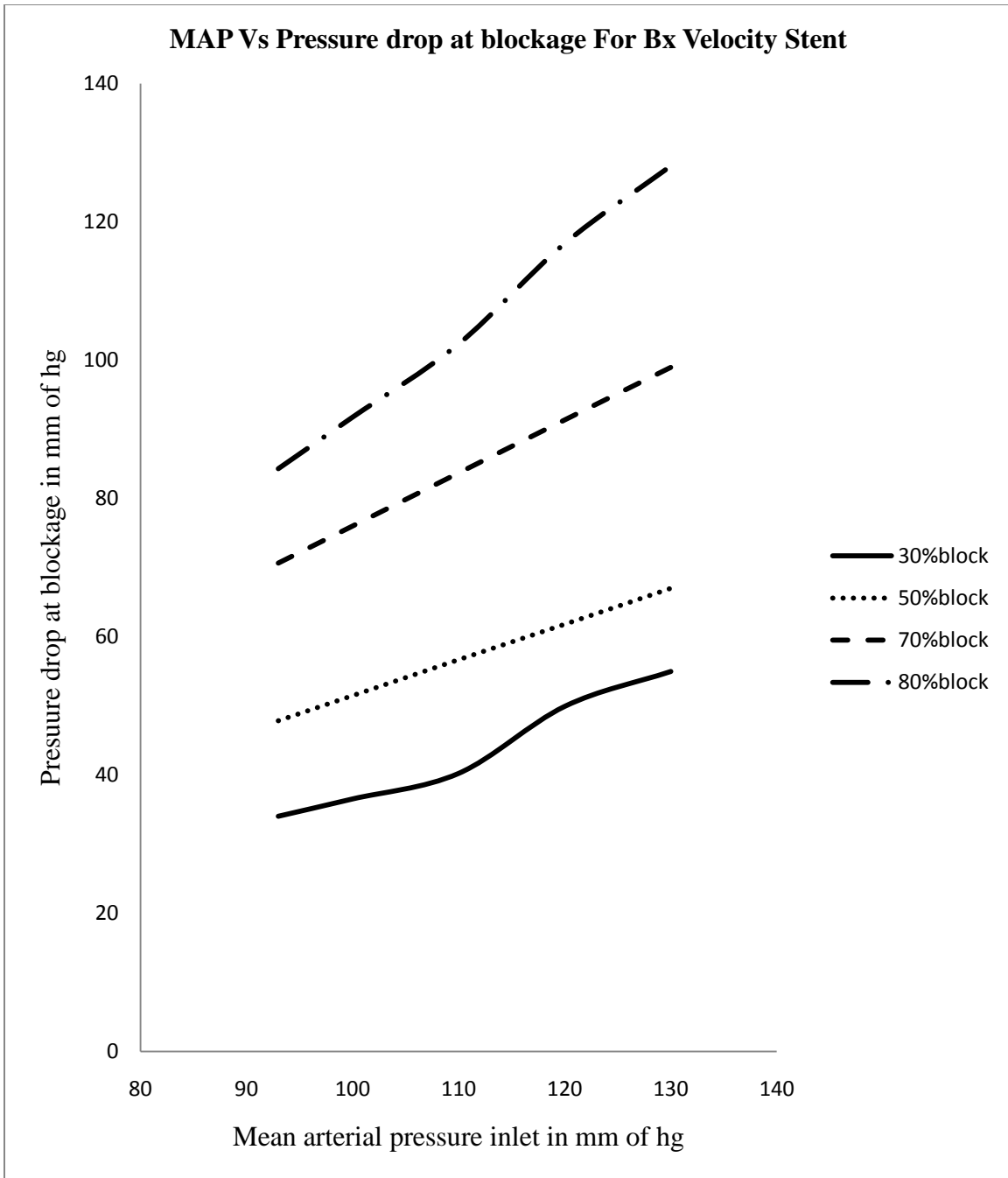
5-2 Contours of Pressure for Fifty Percent Blockage



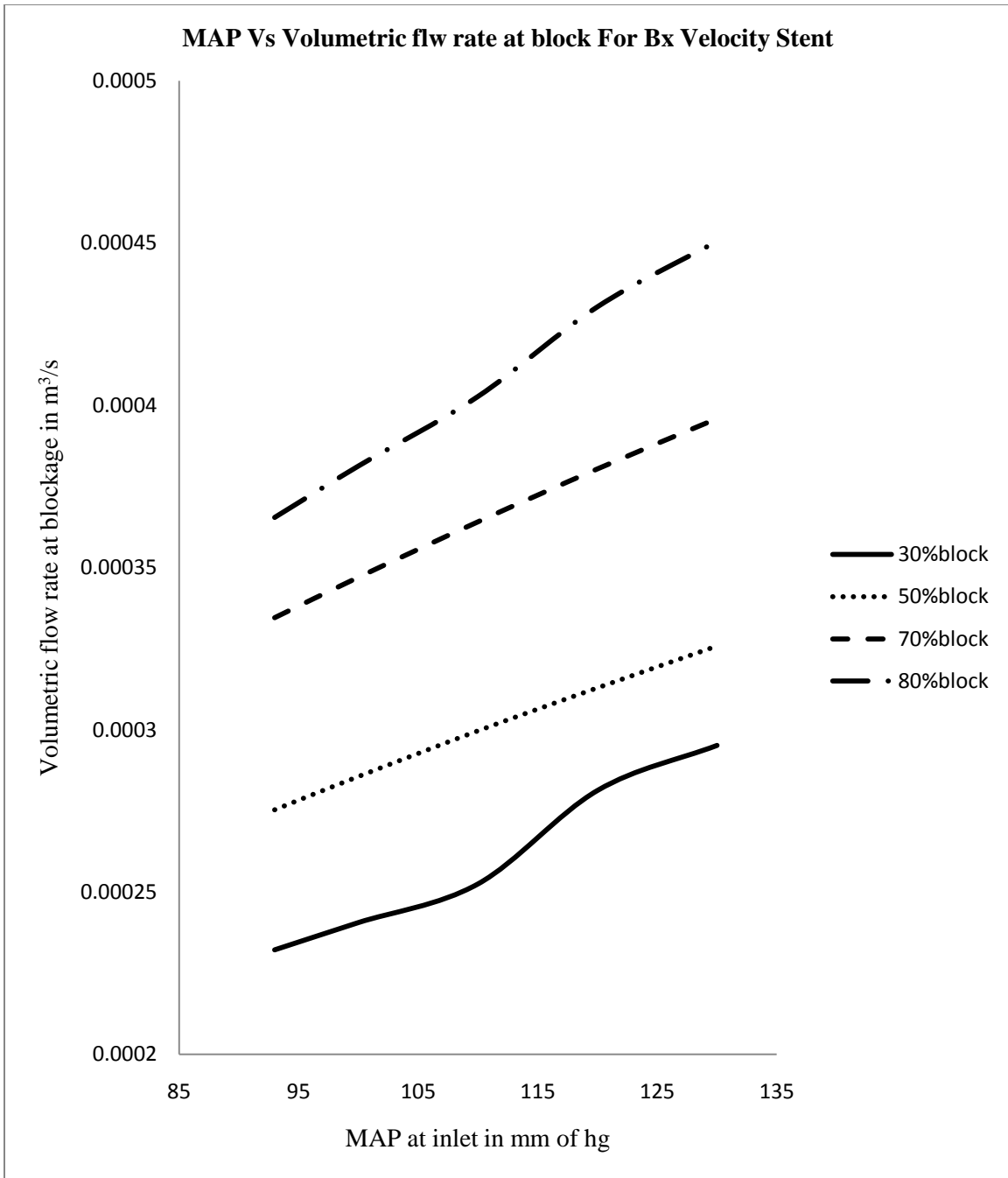
5-3 Contours of Pressure for Seventy Percent Blockage



5-4 Contours of Pressure for Fifty Percent Blockage



5-5 Pressure Drop For Bx Velocity Stent

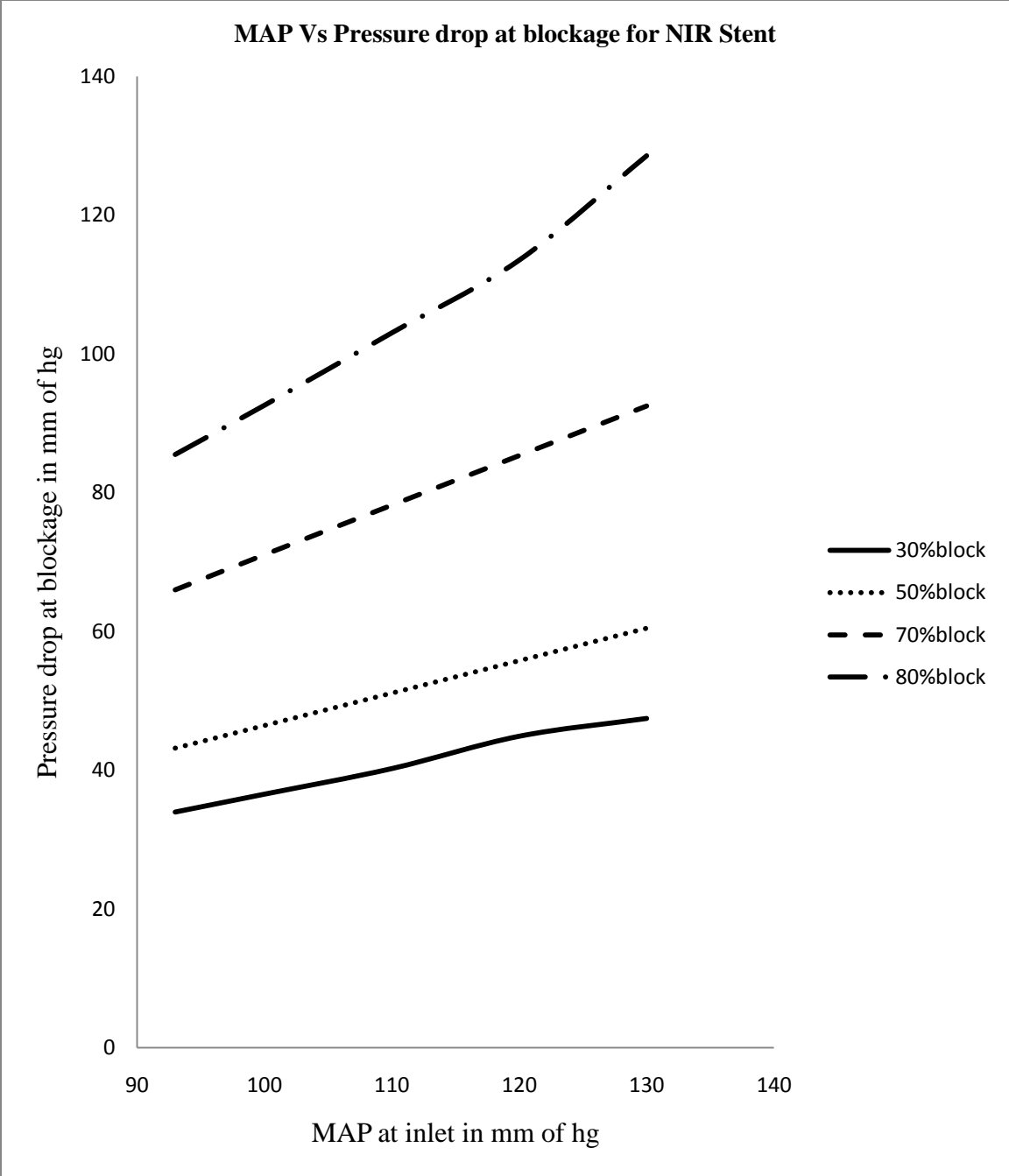


5-6 Volumetric Flow rate For Bx Velocity Stent

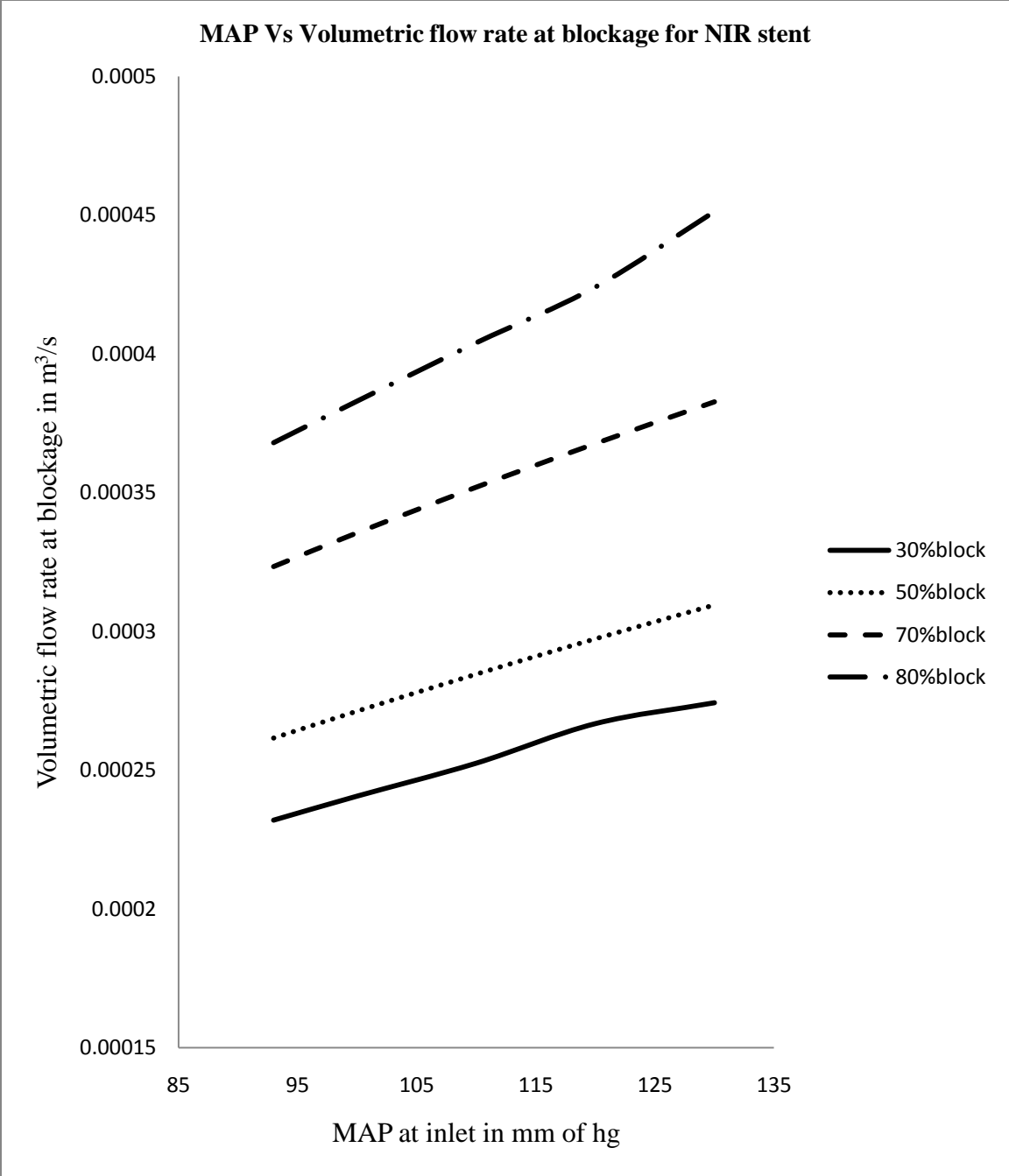
A similar analysis is performed using NIR Stent to determine the pressure drop and volumetric flow rate at different blockage rates. For a mean arterial pressure inlet pressure drop is high for a highly blocked stented artery (Figure.5-7). However the results obtained at the outlet are in contrast to the one at the blockage due to the difference in geometry at that region.

Similar to Bx velocity stent, volumetric flow rate of NIR Stent increases with increase in blockage rate (Figure.5-8). In contrast to the stenosed region the volumetric flow rate at outlet of stented artery decreases with increase in blockage rate.

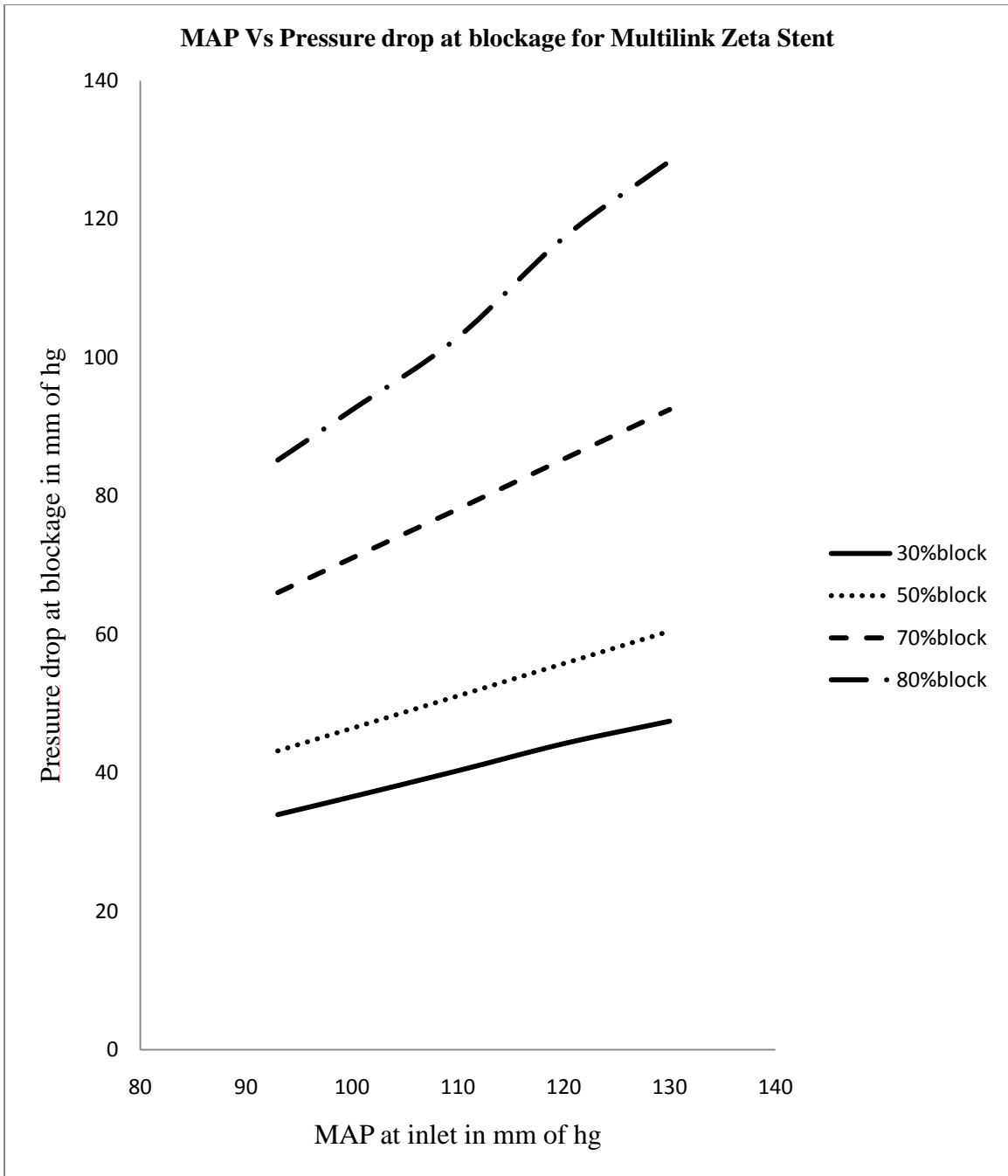
Similar to Bx velocity and NIR stents, volumetric flow rate and pressure drop of Multilink Zeta stent increases with increase in blockage rate (Figure.5-9 & 5-10). In contrast to the stenosed region the volumetric flow rate at outlet of stented artery decreases with increase in blockage rate.



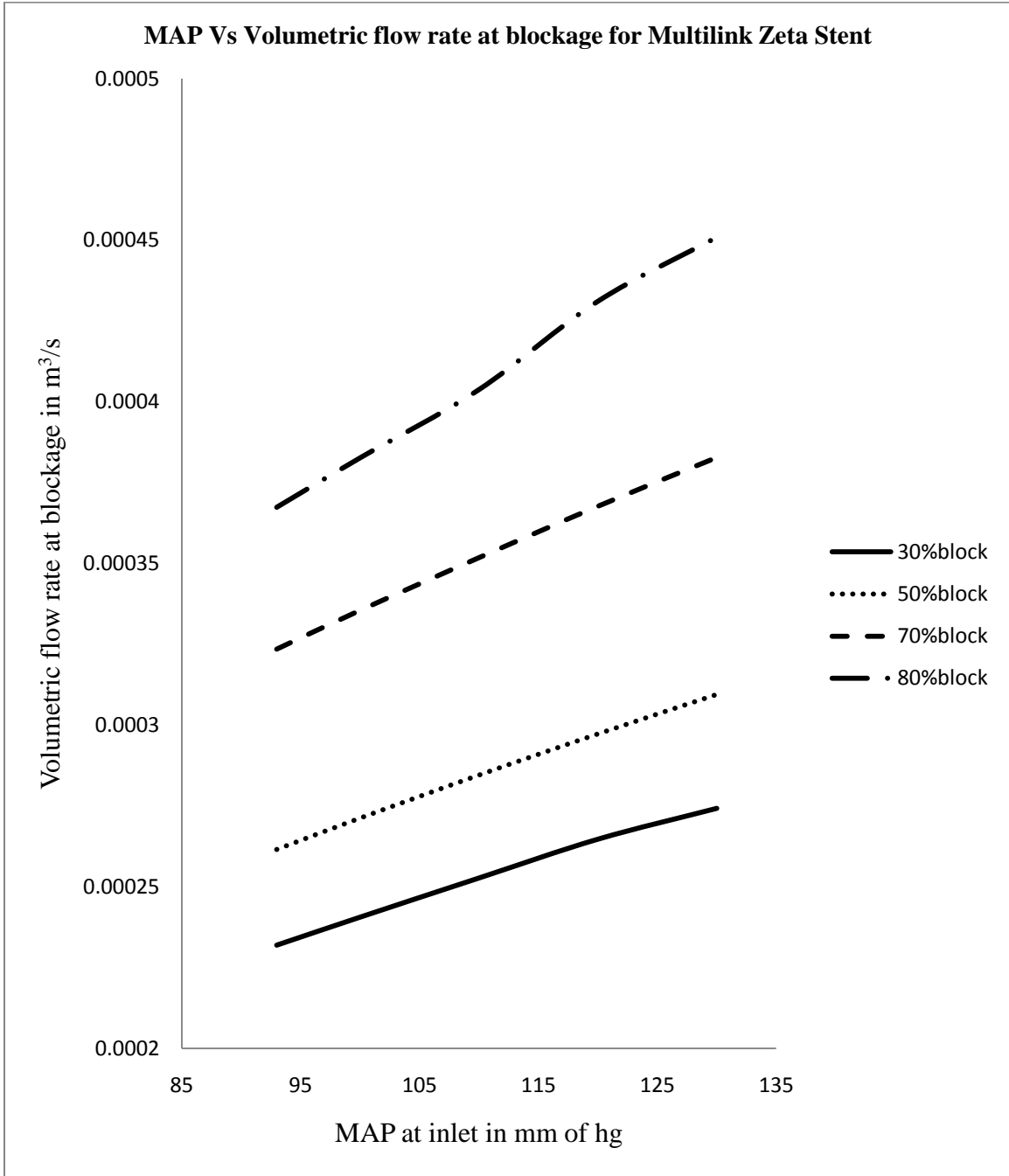
5-7 Pressure Drop For NIR Stent



5-8 Volumetric Flow rate For NIR Stent



5-9 Pressure Drop For Multilink Zeta Stent



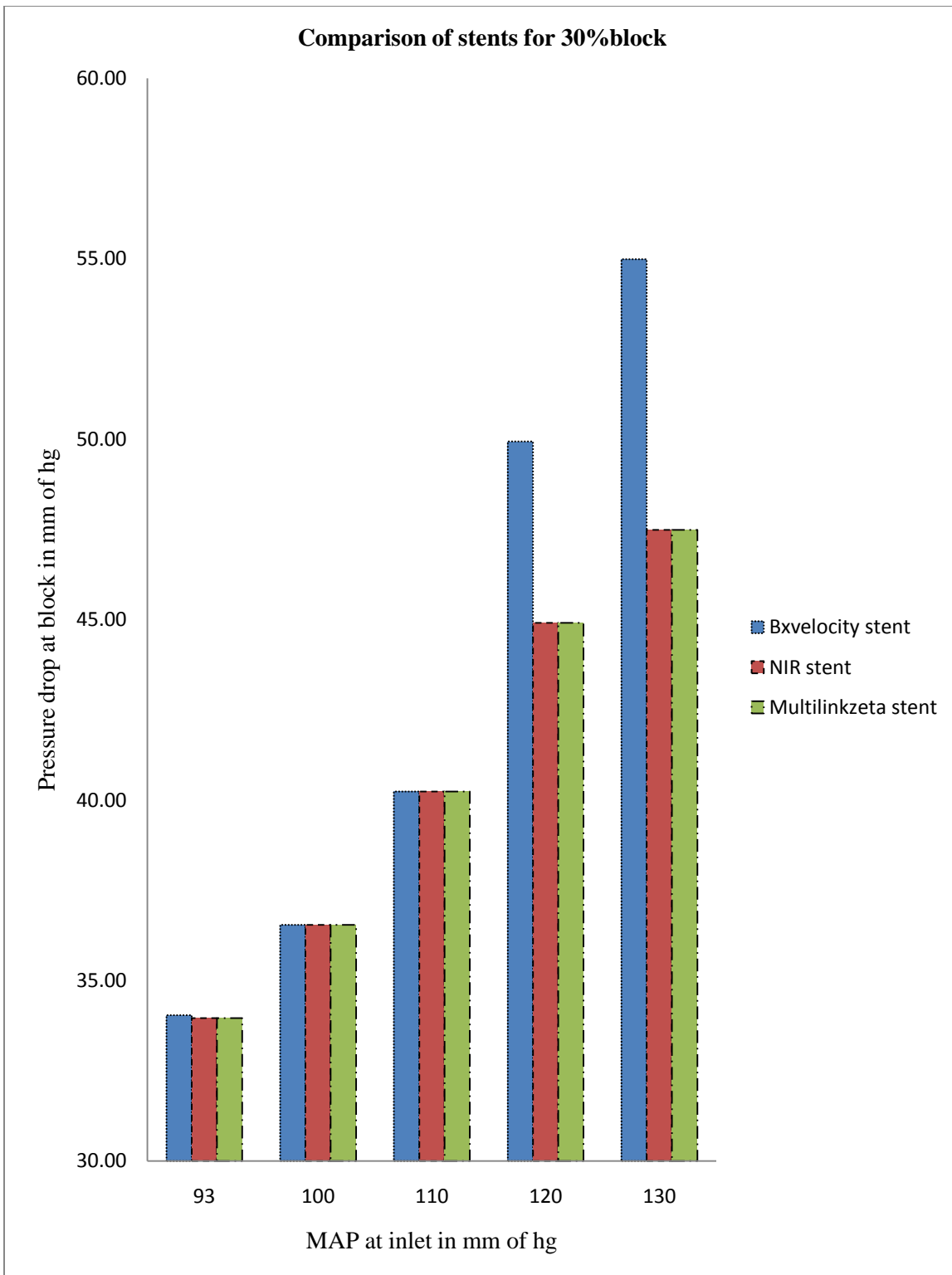
5-10 Volumetric Flow rate For Multilink Zeta Stent

The results obtained from Bx velocity, NIR Stent, Multilink Zeta Stent at thirty percent blockage helps in determining the efficiency of a stent. At high blood pressure stage 1 and 2 the pressure drop is very high for Bx velocity stent when compared to NIR and Multilink Zeta stent which shows that NIR and Multilink zeta stent were more efficient than Bx Velocity stent (Figure.5-11).

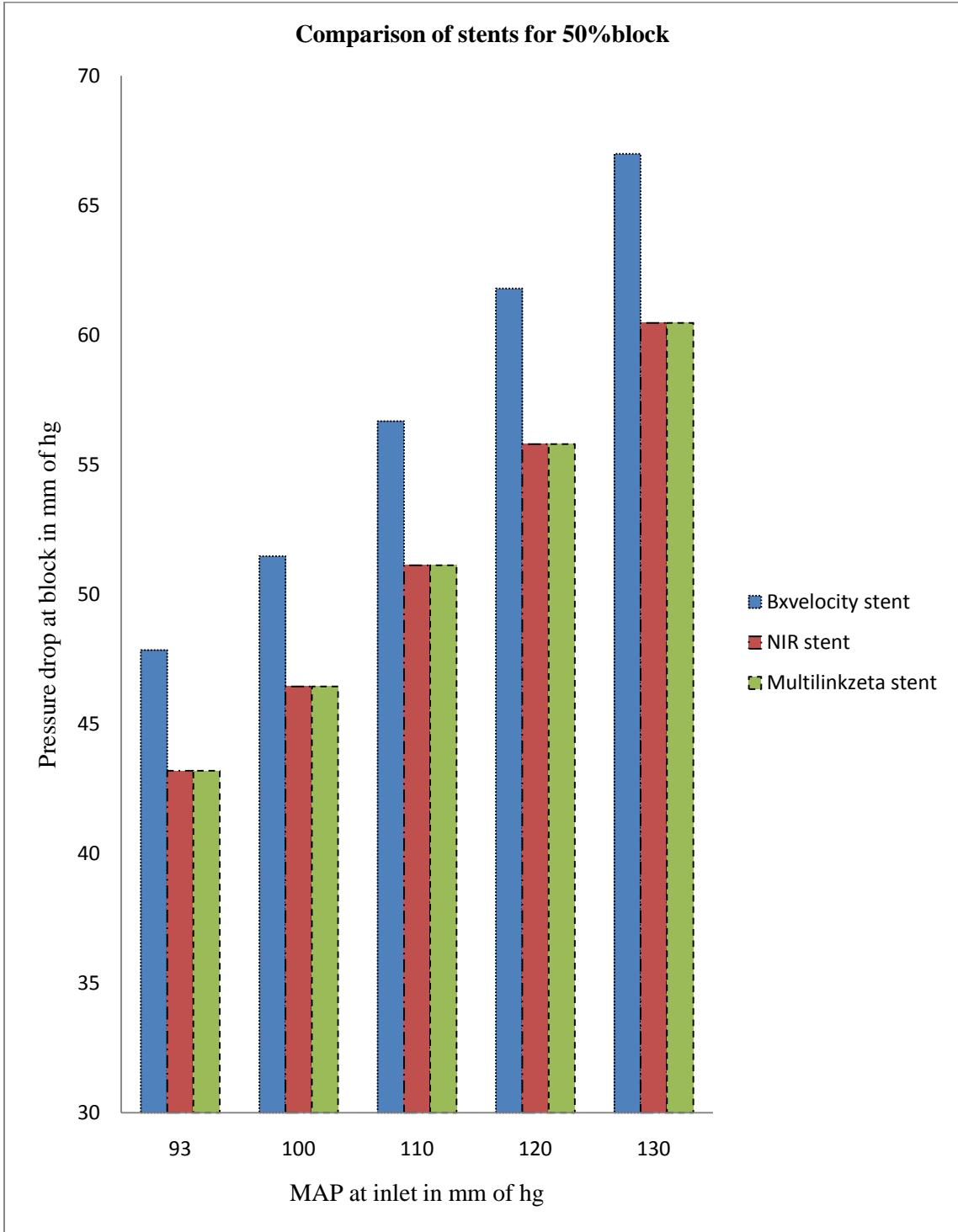
The pressure drops at all the stages of blood pressures were high in case of Bx Velocity stent with fifty percent stenosis. The other two stents showed significantly similar pressure drops but low values when compared to Bx Velocity stent. This shows that NIR and Multilink Zeta stents are more efficient than Bx Velocity stent (Figure.5-12).

Similar trends of results were obtained at seventy percent blocked artery and thus NIR and Multilink zeta stents are more efficient than Bx velocity stent at all the stages of blood pressures (Figure.5-13).

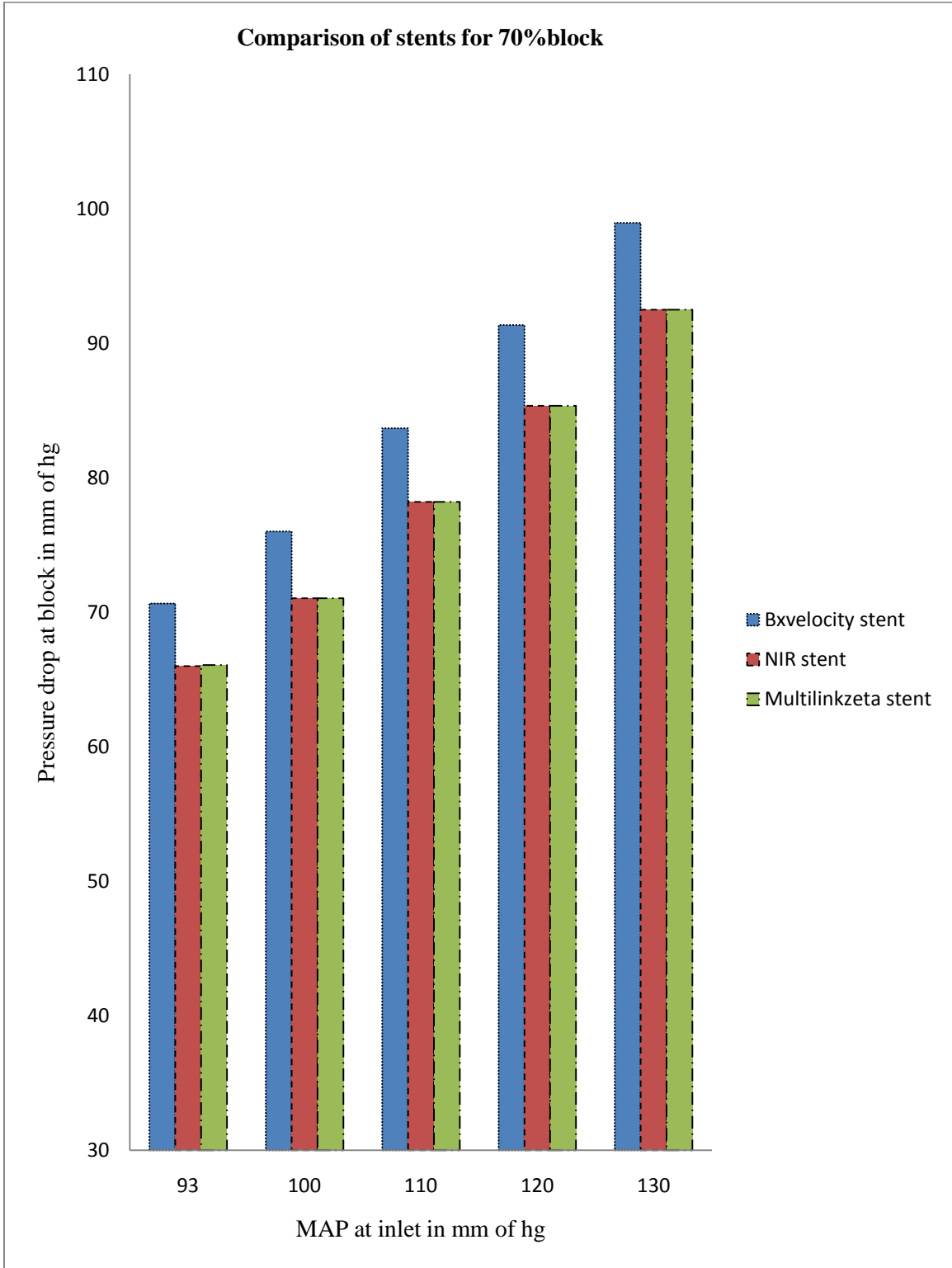
In case of eighty percent stenosis the pressure drop is high for both Bx Velocity and Multilink zeta stents for all the stages of blood pressures. The pressure drop is very low at all the stages of blood pressure when NIR stent exists which shows that under critical circumstances of stenosis NIR stent is highly optimum when compared to other stents (Figure.5-14).



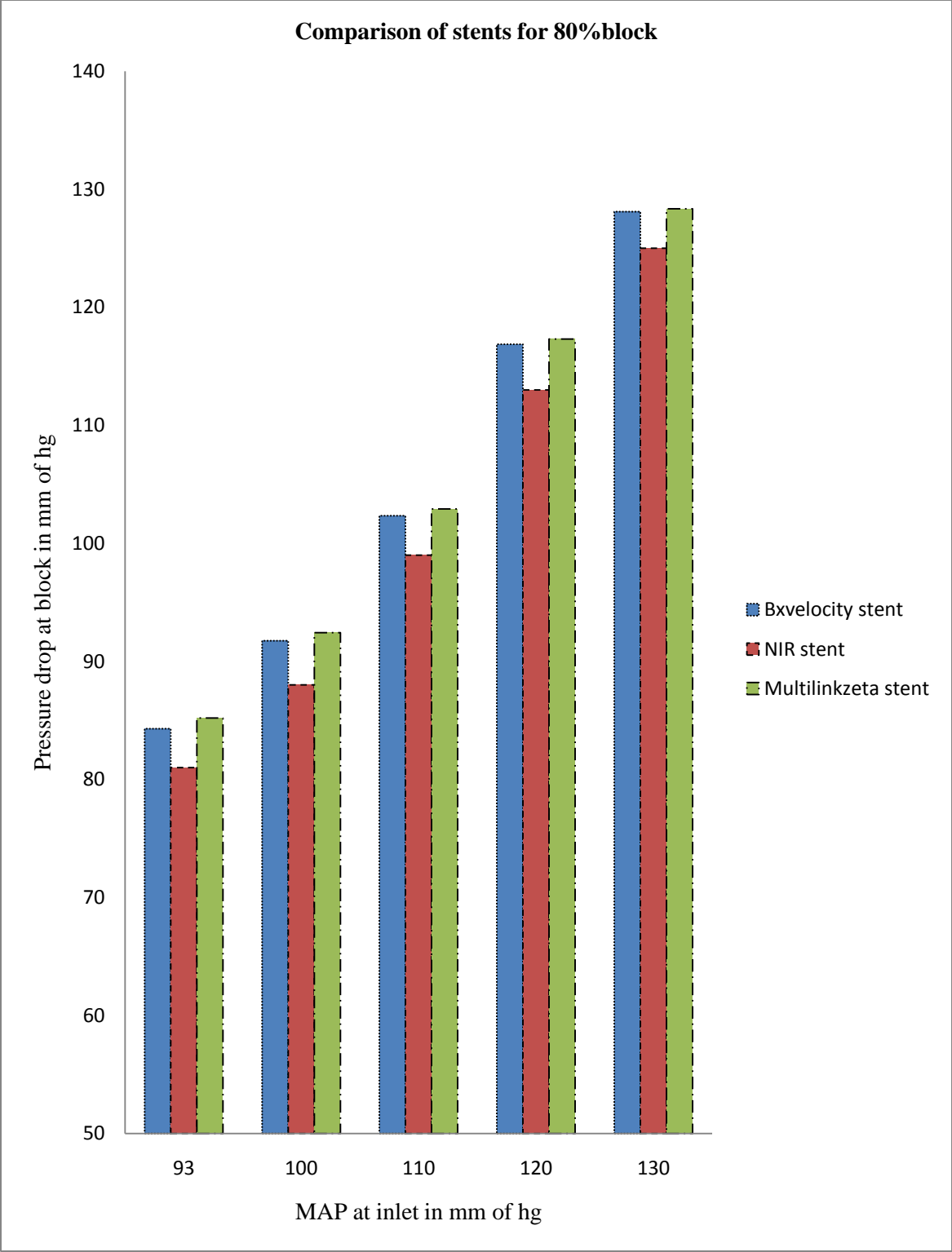
5-11 Pressure Drops for Thirty Percent Blockage



5-12 Pressure Drops for Fifty Percent Blockage



5-13 Pressure Drops for Seventy Percent Blockage

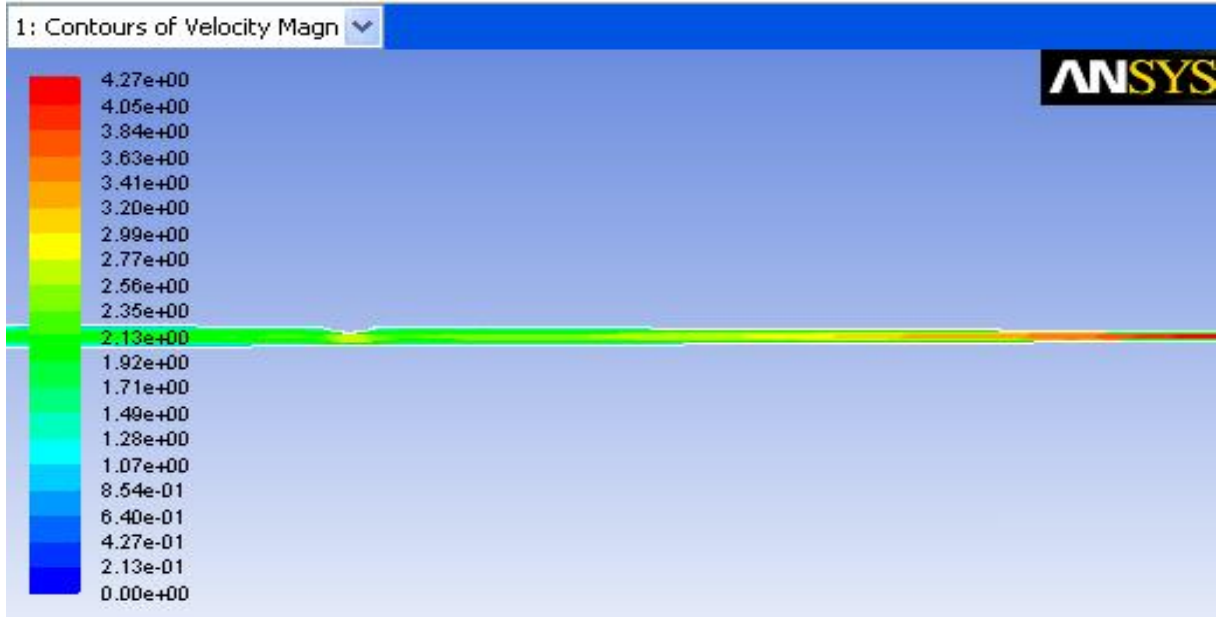


5-14 Pressure Drops for Eighty Percent Blockage

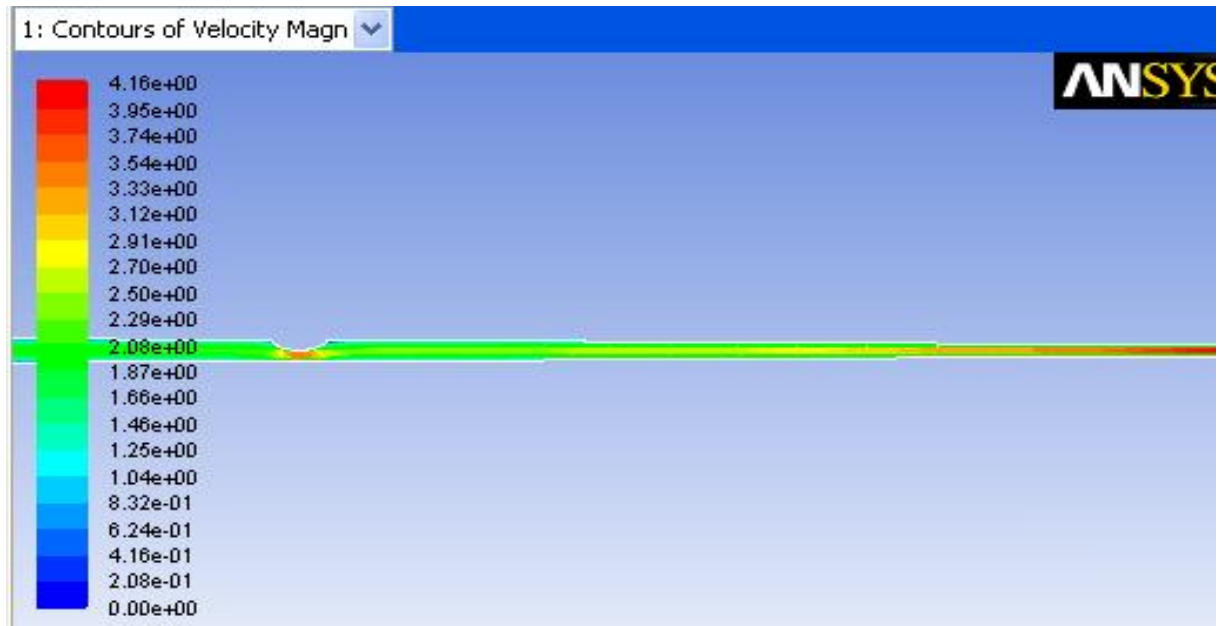
From the figure it is observed that for an unsteady flow analysis the velocity is highest at the outlet of a thirty percent blocked artery when compared to blocked region [Figure.5-15]. In a fifty percent blocked artery, the velocities at the blockage and outlet are same because the geometries are same in both the regions [Figure.5-16]. In case of the remaining blockage levels of seventy and eighty the velocities at the blockages are high when compared to outlet [Figure.5-17 & 5-18].

Since NIR stent is proved to be highly efficient when compared to other stents unsteady flow conditions are applied to obtain the results at the outlet of the artery. A user defined function is written in post processor using mean arterial pressure inlet. The velocity at the outlet is high for an inlet pressure (high blood pressure stage 2). Similar trends of results were obtained at all the stenosis levels in NIR stented artery. Due to the narrow region at outlet the velocity at the outlet is high for thirty percent blockage when compared to fifty, seventy and eighty (Figure.5-19 to 5-22).

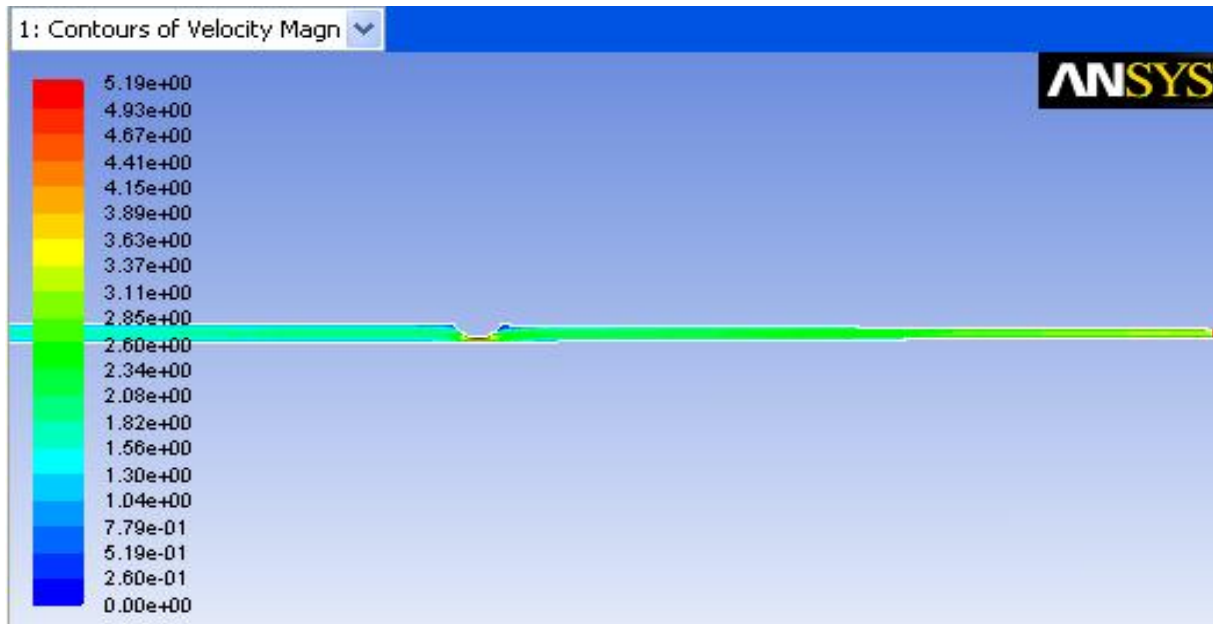
The velocity at the outlet for an unsteady blood pressure stages as inlet is compared to steady state flow conditions. The obtained results show that the velocity is high for an unsteady flow rate when compared to steady flow rates. Similarly the mass flow rates at the outlet were high for an unsteady blood flow when compared to steady flow (Fig.5-23 & 5-24).



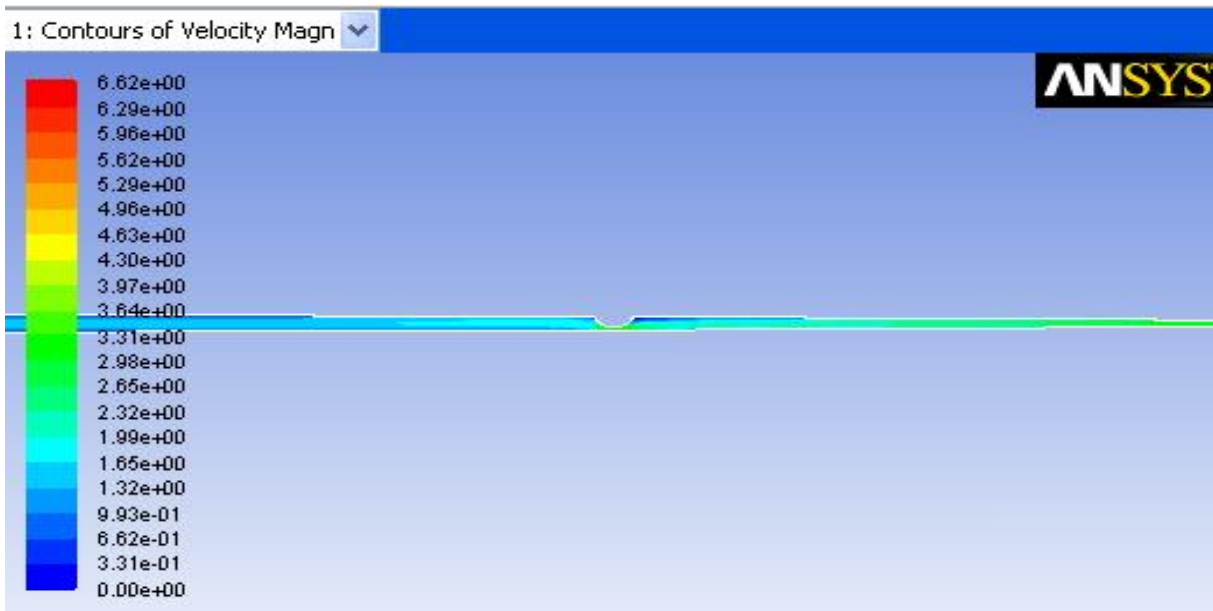
5-15 Contours of Unsteady Velocity for Thirty Percent Blockage



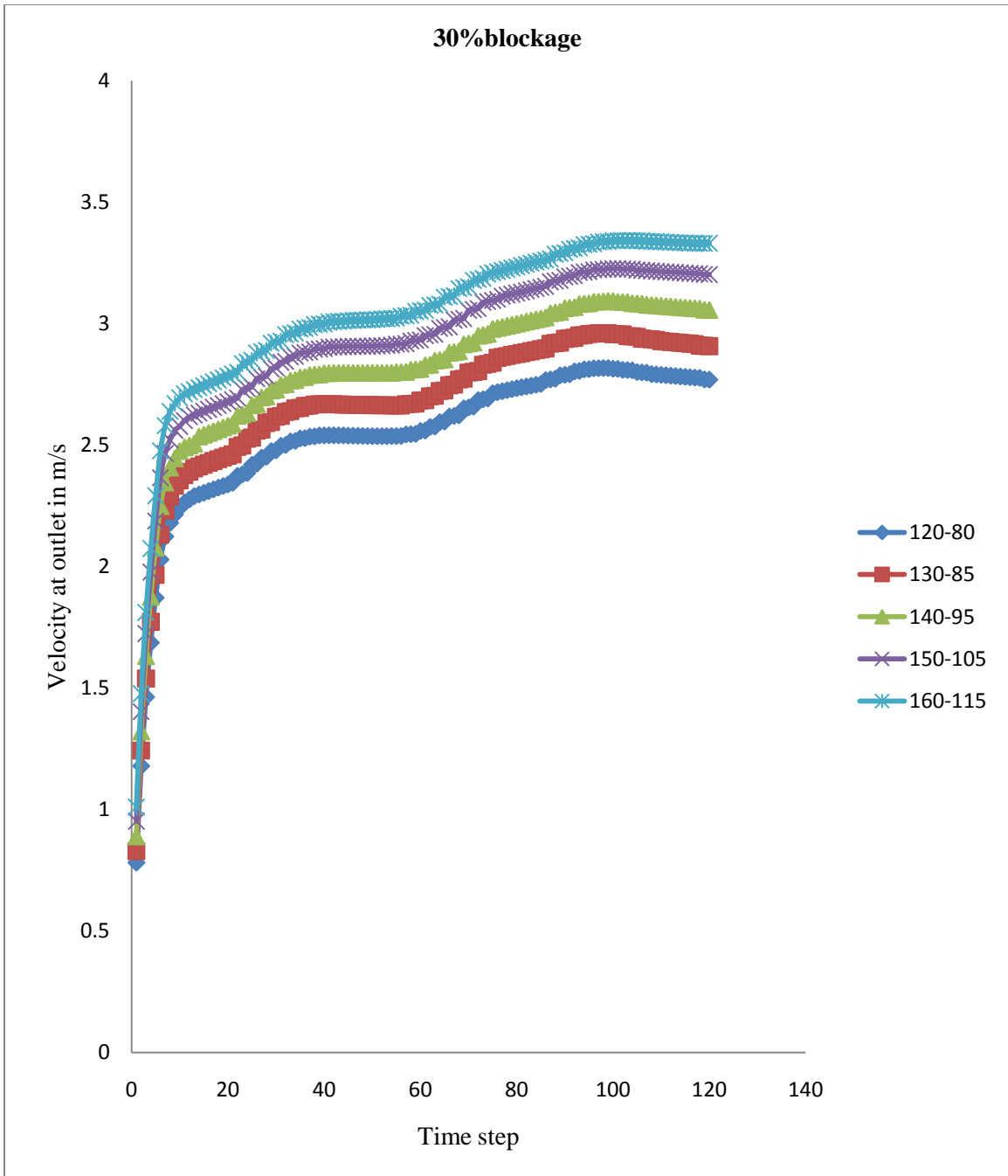
5-16 Contours of Unsteady Velocity for Fifty Percent Blockage



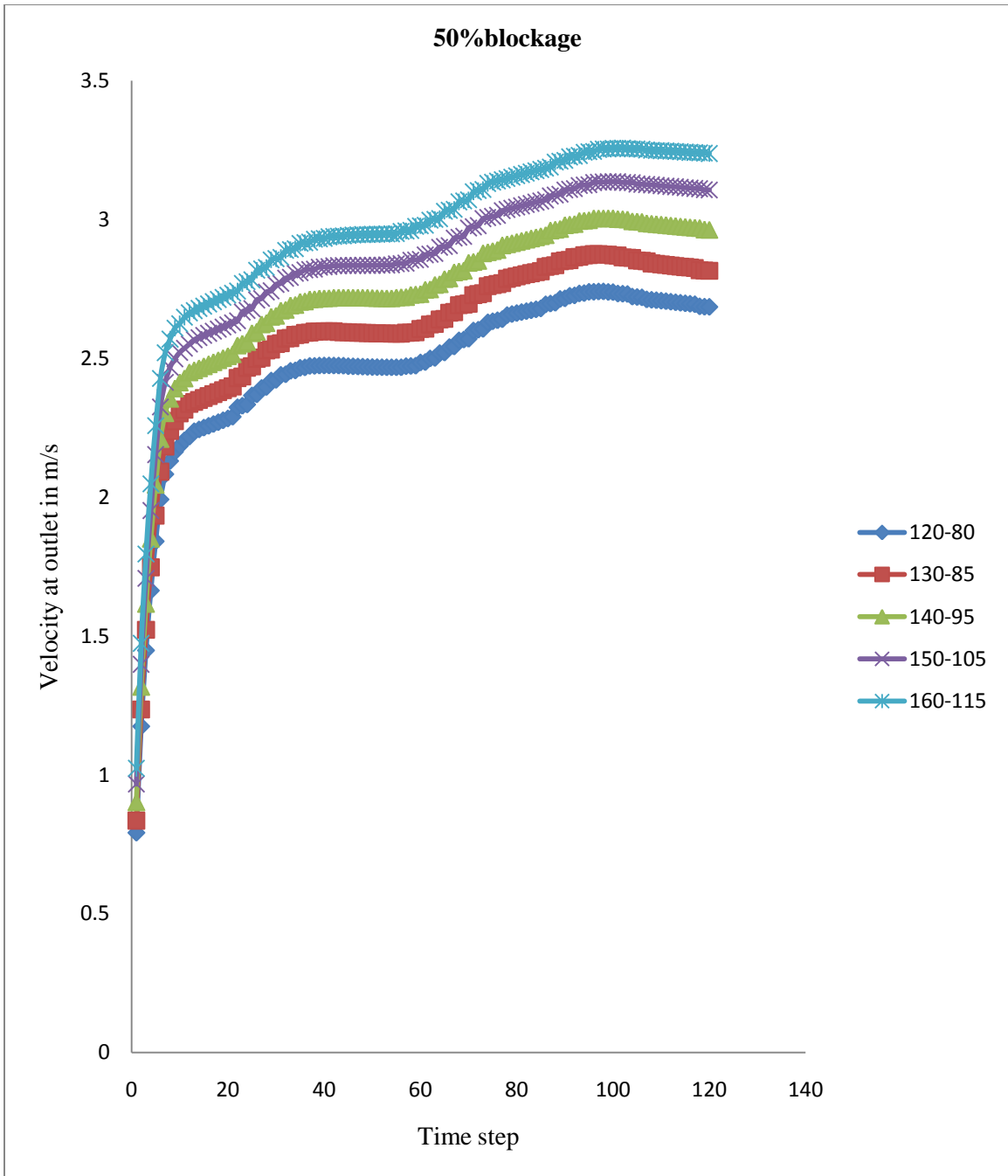
5-17 Contours of Unsteady Velocity for Seventy Percent Blockage



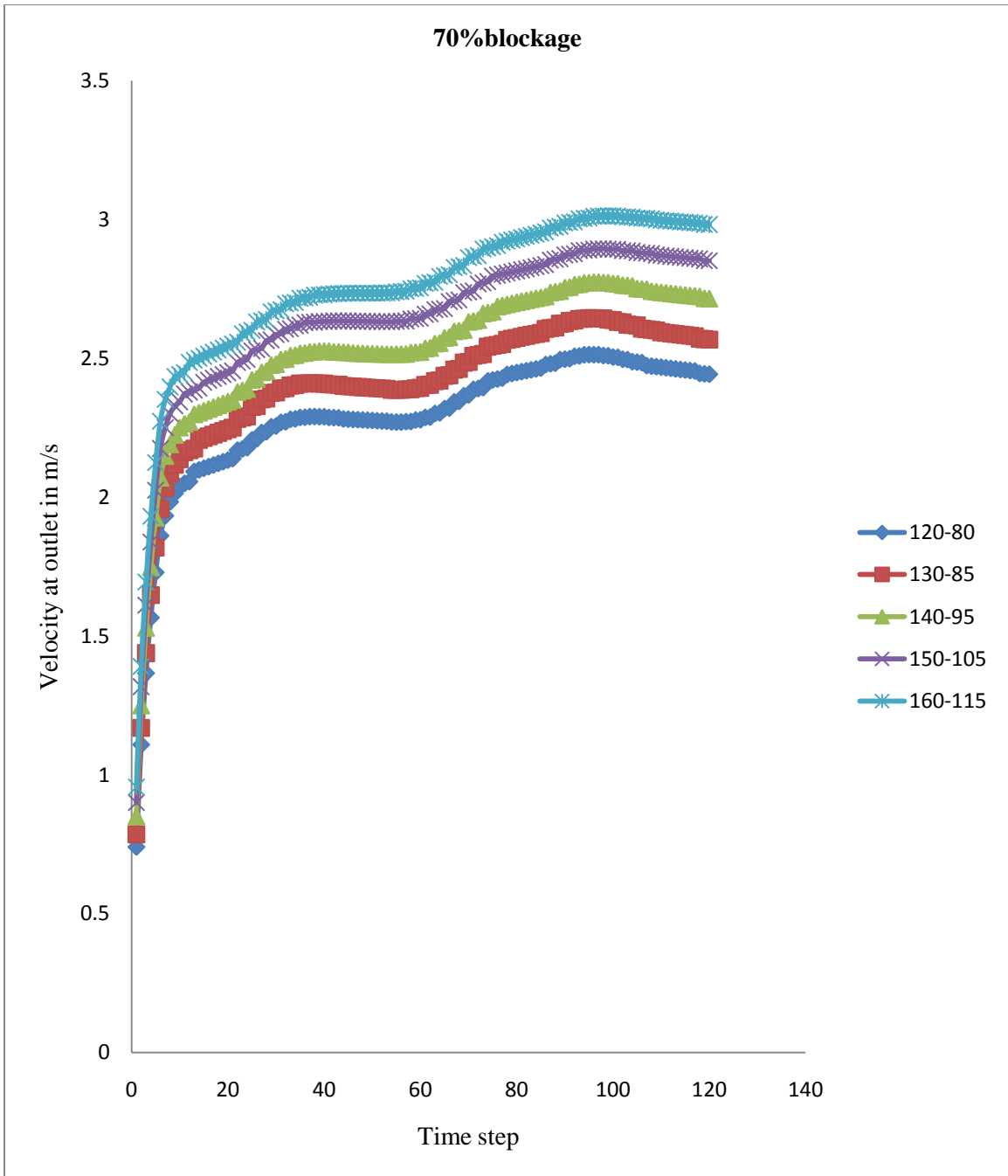
5-18 Contours of Unsteady Velocity for Eighty Percent Blockage



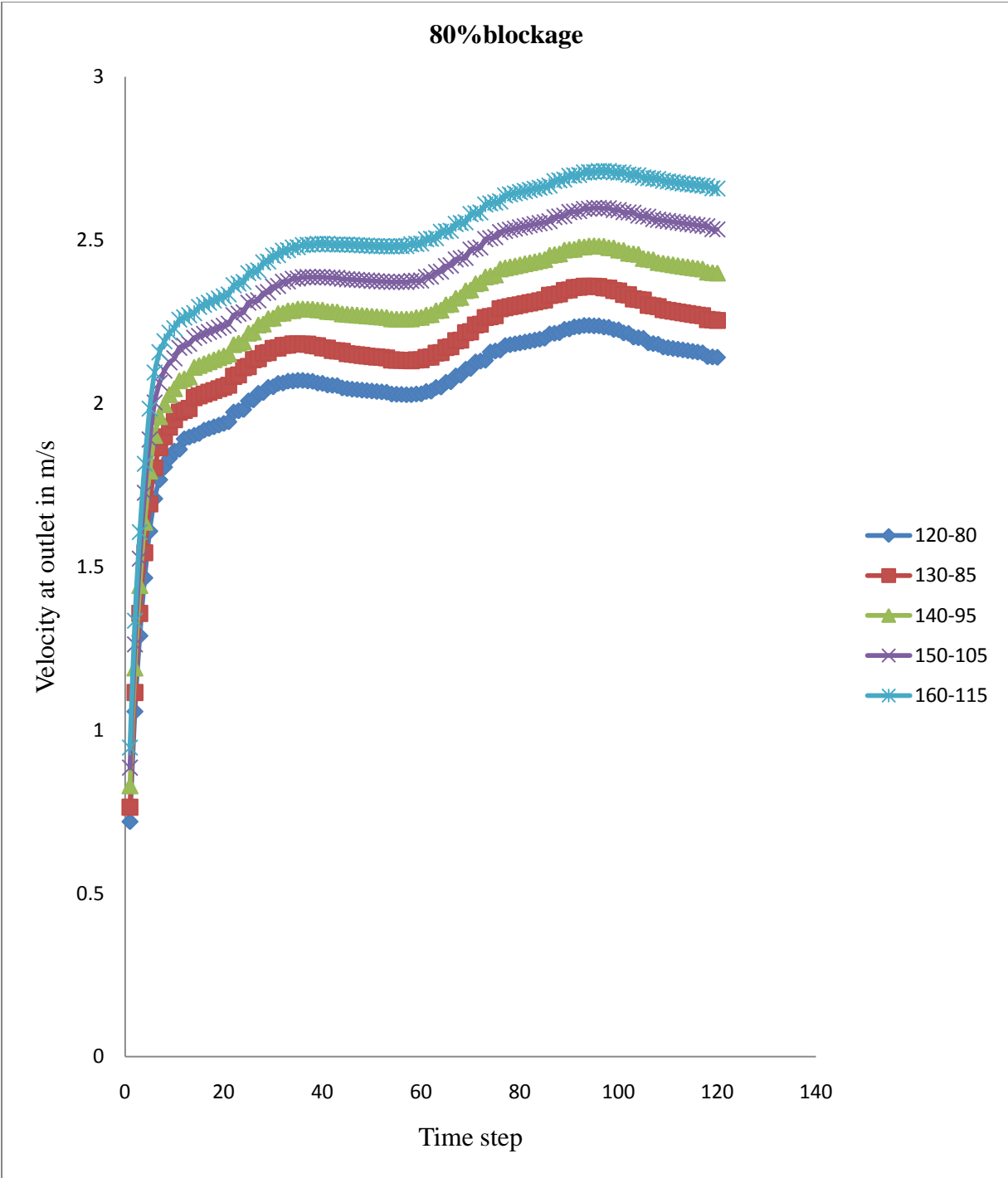
5-19 Unsteady Velocity Outlet at Thirty Percent Blocked Artery



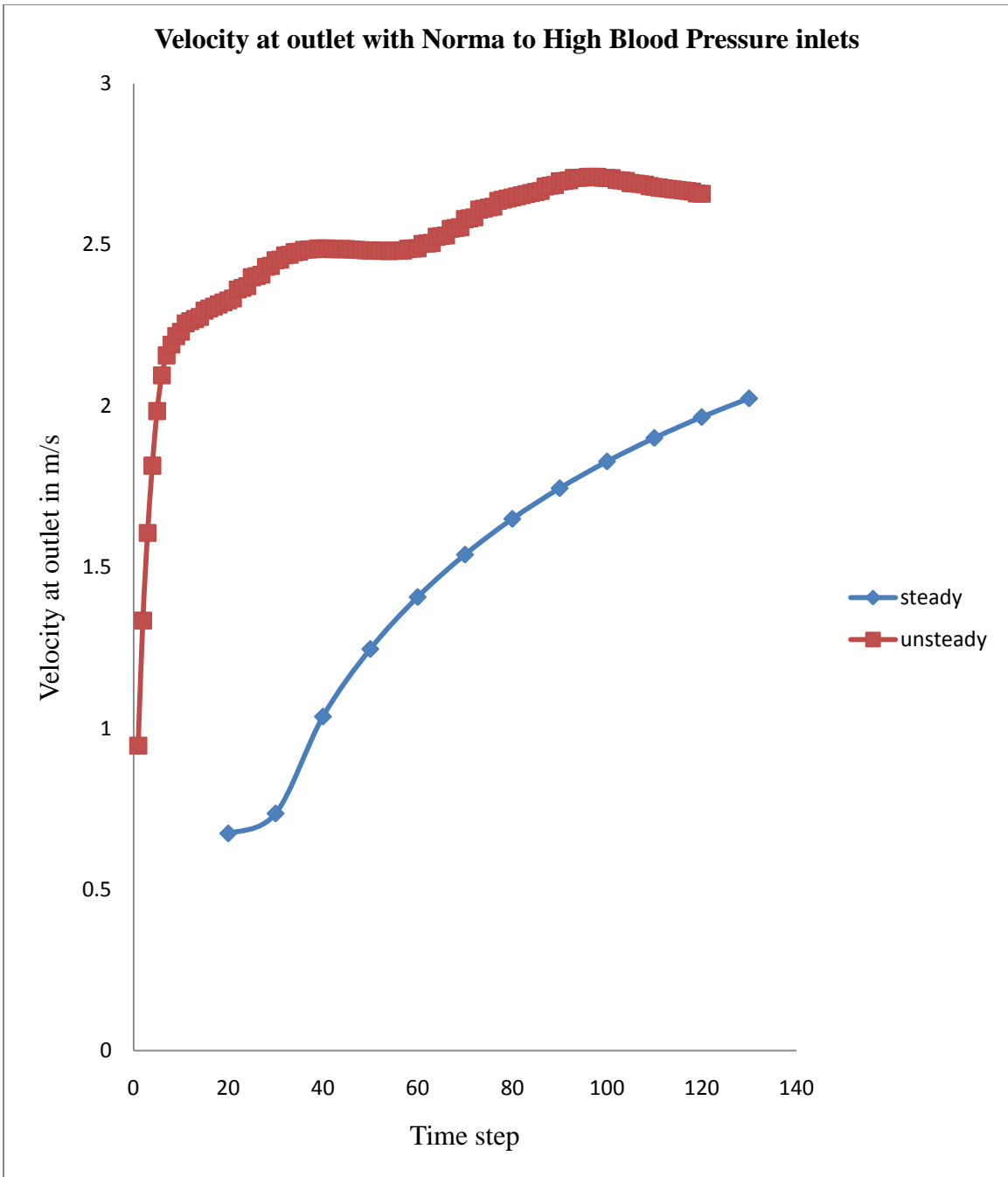
5-20 Unsteady Velocity Outlet at Fifty Percent Blocked Artery



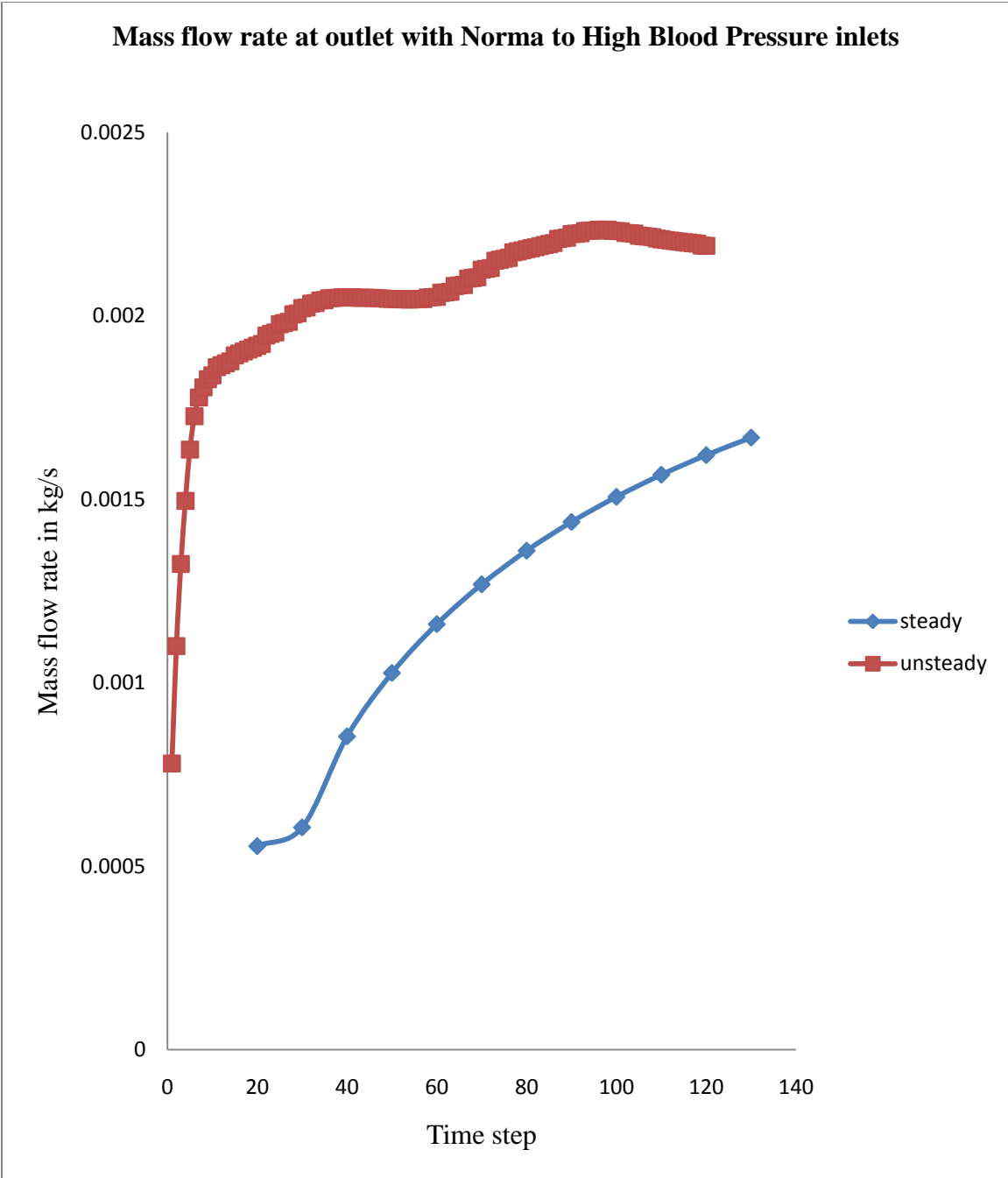
5-21 Unsteady Velocity Outlet at Seventy Percent Blocked Artery



5-22 Unsteady Velocity Outlet at Eighty Percent Blocked Artery



5-23 Velocity at Outlet of Artery



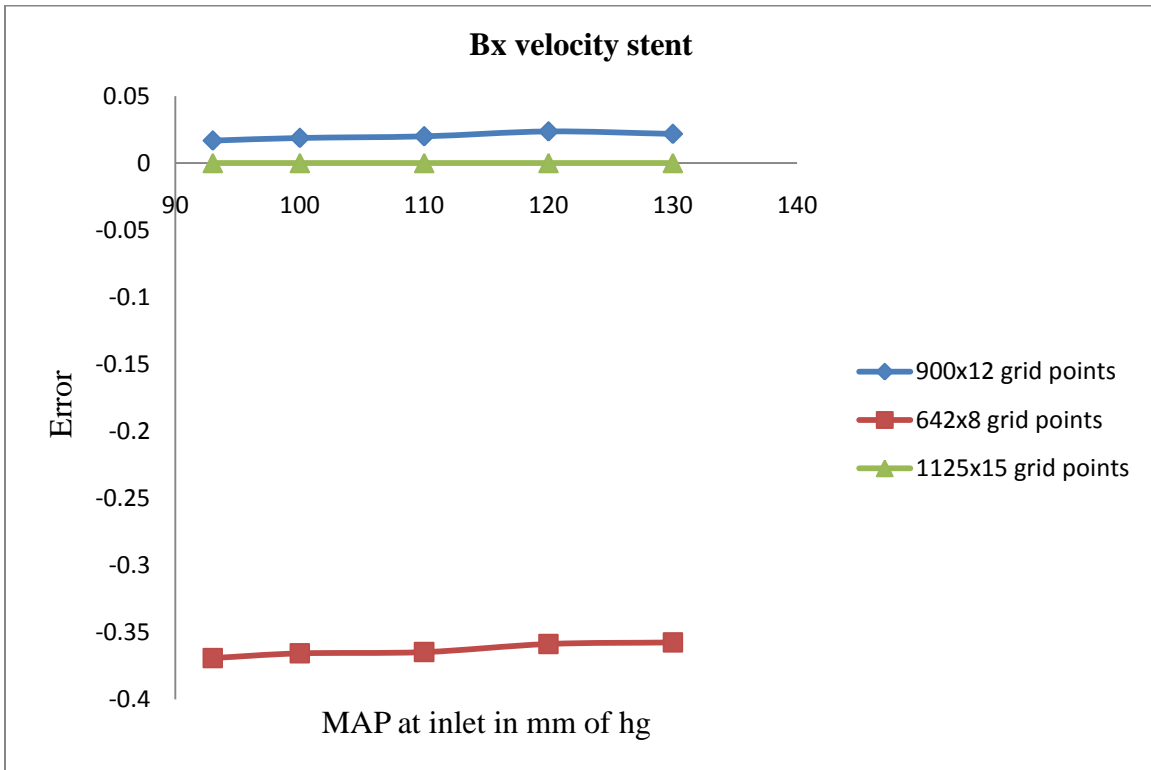
5-24 Mass Flow Rate at Outlet of artery

5.2 Grid Independence

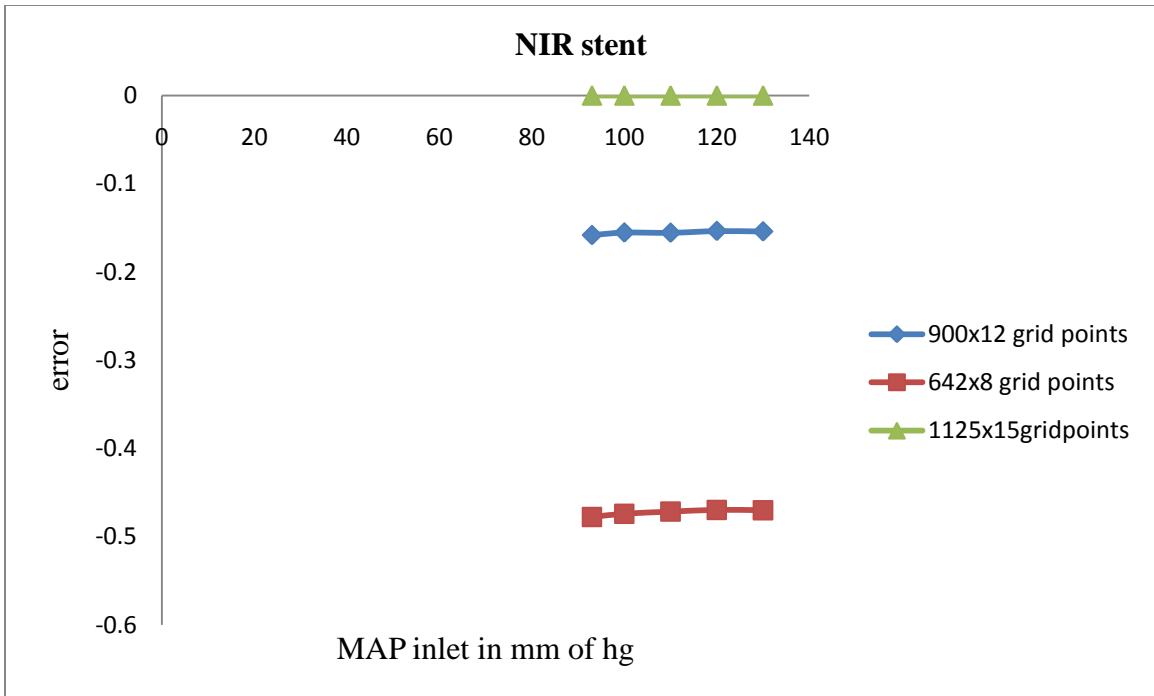
In finite volume method, a number of different grid sizes will be considered to check the sufficiency of mesh resolution. In the present study, three different uniform mesh sizes are considered which are measured based on the number of grid points. The mesh sizes are taken as 900 x 12(900 axial and 12 radial), 642 x 8 and 1125 x15 and compared to estimate the error based on coarse and fine grid.

$$\text{Error} = \frac{\Delta P_{\text{coarse}} - \Delta P_{\text{fine-mesh}}}{\Delta P_{\text{fine-mesh}}}$$

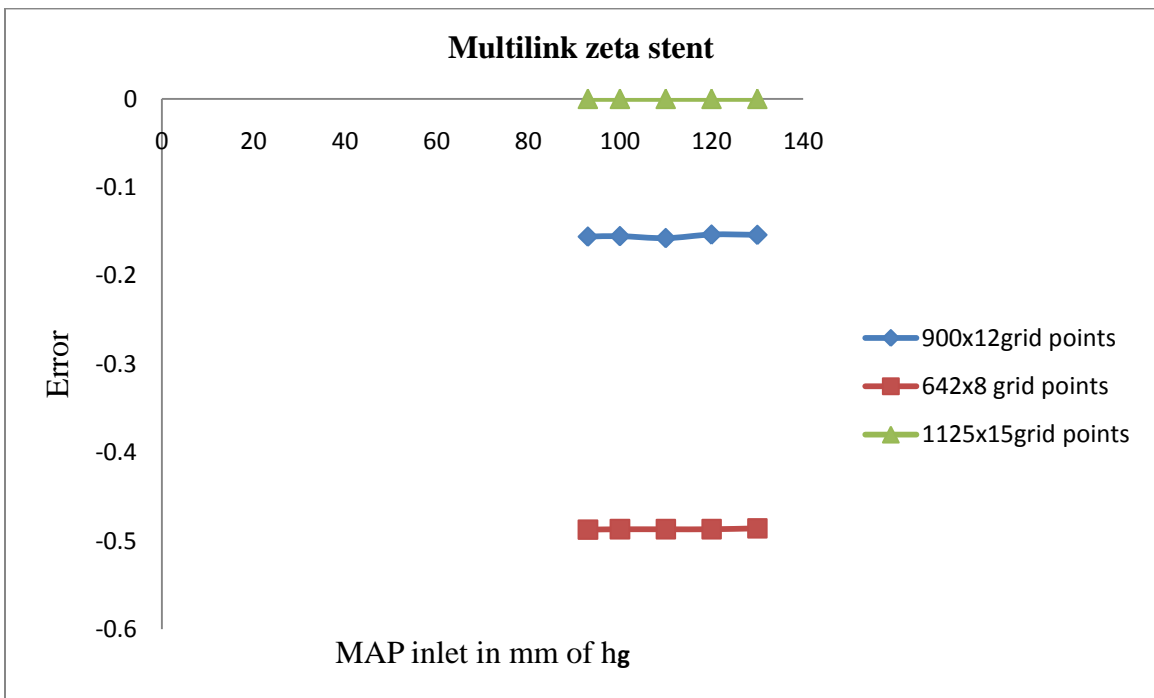
ΔP is the pressure drop in the stented artery and required calculations are done based on the above formula. From the calculations, the mesh density at 1125 x 15 grid point showed no percentage error. The results showed high accuracy at 1125 x 15 grid points for all the three stents (Figure.5-25 to 5-27)



5-25 Grid Independence Check for Bx Velocity Stent



5-26 Grid Independence Check for NIR Stent



5-27 Grid Independence Check for Multilink Zeta Stent

CHAPTER 6

CLINICAL SIGNIFICANCE

The current analysis helps in choosing optimum stent design for the patient suffering with high percent stenosis downstream of stented region. The results obtained can be used for people suffering with various high stages of blood pressures. In addition to these the mass flow rates obtained at the outlet of an artery can be related to the mass flow rates obtained from MRI results. Flow rate of blood should be uniform since they send blood to heart and receive blood from heart. The results illustrate that there will be lack of blood supply to heart during certain period of time which might lead to heart strokes. Therefore proper care can be taken to improve the blood flow rate under certain circumstances of stenosis downstream of stented region. Efforts can be made to decrease the blood pressure rate depending upon the stage at which the patient is suffering. Stents cannot be placed in a 2mm and 1mm artery and hence other surgical methods can be chosen to improve blood flow.

CHAPTER 7

CONCLUSIONS AND FUTURE RECOMMENDATIONS

7.1 Conclusions

The current research is mainly concerned with the hemodynamic, pressure and velocity analysis of blocked artery downstream of stented region. A steady blood flow analysis is performed through a partially blocked artery downstream of stented region at different stages of blood pressures. With an increase in mean arterial pressure the pressure drop and volumetric flow rates increases for a highly blocked stenosed artery. In addition most commonly used FDA stents are analyzed and from the results it is proved that for a highly blocked stenosed artery NIR stent showed higher efficiency than the remaining two. Since flow inside a human artery is unsteady, pulsatile blood flow is carried out in a stenosed artery downstream of NIR stent. Compared to steady, unsteady mass flow rate and velocity showed significant results at different time steps of flow. The geometry at the outlet of the artery is responsible for a high velocity at the outlet for thirty percent blockage when compared to fifty, seventy and eighty. If a comparison is to be made for different inlet blood pressure levels, the velocity and mass flow rates are quite high at the outlet for high blood pressure stage 2. Grid independence is achieved to check the accuracy of mesh resolution.

7.2 Future Recommendations

The following are some of the suggestions for future work

- A three dimensional analysis can be done on stented artery during flow downstream.
- The mesh density at stent region can be increased to observe the flow rate more accurately.
- There are few other FDA approved stents and the optimum stent among them can be compared with NIR stent.
- The present study included only steady flow analysis while comparing the stents, hence for future work unsteady results can also be used to obtain efficient stent geometries.
- Drug eluting stents are being frequently used in the present days thus these stents can be used in the stented artery with a partial blockage downstream of stented region.
- The current analysis obtained results at various stages of blood pressure but along with this, major changes can also be observed in diabetic patients. Thus future analysis can be done on diabetic patients.

LIST OF REFERENCES

REFERENCES

1. Fuster V. Atherosclerosis, thrombosis and vascular biology. In: Goldman L, Ausiello D, eds. Cecil Medicine. 23rd ed. Philadelphia, 2007, chap 69.
2. Retrieved on 03/10/2011 at : <http://www.nhlbi.nih.gov/health/dci>
3. Retrieved on 03/1/2011 at: <http://www.webmd.com/cholesterol-management/treatments-for-advanced-atherosclerosis>
4. Heart and Stroke Facts, and Stent Procedure, Book from American Heart Association, 2002.
5. Retrieved on 03/1/2011 at: <http://www.ebaptisthealthcare.org/StrokeCare/Prevention3.aspx-stent> image
6. Retrieved on 03/1/2011 at: http://www.texashealth.org/heartV_template_tertiary.cfm?id=4065-3 stent image
7. Retrieved on 03/1/2011 at: <http://www.liveingoodhealth.info/article/a-look-at-some-of-the-diseases-caused-by-streptococcus-bacteria/-coronary-artery-disease>
8. Retrieved on 03/1/2011 at: <http://www.cardiosmart.org/HeartDisease/CTT.aspx?id=202-carotid-artery-stenting>
9. Retrieved on 03/1/2011 at: http://www.nhlbi.nih.gov/health/dci/Diseases/arm/arm_types.html-aortic-aneurysm
10. Retrieved on 03/1/2011 at: <http://thejqcorner.wordpress.com/2010/12/24/prayer-does-it-work/-coronaryartery-bypass>
11. Retrieved on 03/1/2011 at: http://www.multiplesclerosisconnect.com/healthcenter/documents/hw108781?section=hw108781-sechttp://www.chainonline.org/content.cfm?content_id=1185-thrombosisafter-stent-implantation
12. Andreas.O, Peter.W and James.E, “Computational Fluid Dynamics and stent design,” International Society of Artificial Organs, vol.26, pp.614-621,2002.
13. John.F , Douglas.A, Lars.E, Ismail.G, Judy.R, David.C and Paul.S, “Three dimensional Computational Fluid Dynamics Modeling of alterations in coronary wall shear stress

- produced by stent implantation”, *Annals of Biomedical Engineering*, vol.31, pp.972-980,2003.
14. Lucas.H, Clark.A, Michael.R and James.E, “Mechanical modeling of stents deployed in tapered arteries,” *Annals of Biomedical Engineering*, vol.36, pp.2042-2050, 2008.
 15. Weronika.K and Jacek.S, “Numerical Simulation of Restenosis in Stented Coronary Artery”, *World Academy of Science, Engineering and Technology*, vol.58, 2009.
 16. John.F, David.C, Ismail.G, Judy.R and Paul.S, “Stent geometry and deployment ratio influence distributions of Wall Shear Stress: Three-Dimensional Numerical Simulations exploiting properties of an Implanted Stent,” *Bioengineering Conference*, 2003.
 17. Vahab.D, Mohammad.T and Niranjan.S, “Numerical Analysis of Pulsatile Blood Flow in a Stented Human Coronary Artery with a Flow Divider,” *American Journal of Applied Science*, vol. 4, Issue 6, pp.397-404, 2007.
 18. Vahab.D, Mohammad.T and Niranjan.S, “Effect of Stent Geometry on Phase shift between Pressure and Flow Waveforms in Stented Human Coronary Artery,” *American Journal Of Applied Science*, vol.5, Issue.4, pp.340-346, 2008.
 19. Rossella.B, Francesca.G, Francesca.M and Gabriele.D, “Effects of Different Stent designs on local Hemodynamics in Stented Artery”, *Journal of Biomechanics*, vol.41, pp.1053-1061, 2008.
 20. Yong.H, Nandini.D, Andreas.O.F and James.E.M, “Blood Flow in Stented Arteries: A Parametric Comparison of Strut Design Patterns in Three Dimensions”, *Journal of Biomechanical Engineering*, vol.127, 2005.
 21. Rosaire.M, Neil.F and Olivier.B, “3D Numerical Simulations of Stent-Based Local Drug Delivery using Realistic Stent and Vascular Wall Structures,” *Summer Bioengineering Confernce*, pp.25-29, 2003.
 22. Allen J.T, Patrick D.G, Bruce.K, Craig.H, Gerti.T and Renu.V, “A comparison of Flour Stent Designs on Arterial Injury, Cellular Proliferation, Neointima Formation and Arterial Dimensions in an Experimental Porcine Model”, *Catheterization and Cardiovascular Interventions*, vol.53, pp.420-425, 2001.
 23. Minsuok.K, Dale B.T, Markus.T and Hui.M, “Comparison of Two Stents in Modifying Cerebral Aneurysm Hemodynamics”, *Annals of Biomedical Engineering*, vol.36, pp.726-741, 2008.
 24. Won-Pil.P, Seung-Kwan.C, Jai-Young Ko, Anders Kristensson, Al-Hassani.S.T.S, Han-Sung.K and Dohyung.L, “Evaluation of Stent Performances using FEA considering a Realistic Balloon Expansion”, *World Academy of Science, Engineering and Technology*, vol.37, 2008.

25. Sanjay.P, Neil W.B, Alexander I.J.F and Nick.C, “The Influence of Strut-Connectors in Stented Vessels: A Comparison of Pulsatile Flow Through Five Coronary Stents”, *Annals of Biomedical Engineering*, vol.38, pp.1893-1907, 2010.
26. Jonathan.M, Fergal.B, “Comparison of Stent Designs Using Computational Fluid Dynamics”, *Conference Proceeding at School of Mechanical and Transport Engineering*, 2007.
27. Zahora.J, Bezrouk.A, Hanus.J, “Models of Stents-Comparison and Applications, *Physiological Research*, pp.S115-S121, 2007.
28. Gideon P.K and Lazar.M, “Stent Biomaterial and Design Selection Using Finite Element Analysis for Percutaneous Aortic Valve Replacement”, *Artificial Organs*, pp.1525-1594, 2010.
29. FLUENT Version 12.0.7 Manual, 2009.
30. FLUENT Version 12.0.7 User Defined Manual, 2009.
31. Giusepp.S, Gloria.M, Pierfrancesco.A, Clarissa.C, Fabrizio.C, Paolo.R, Renu.V and Antonio.C, “Engineering Aspects of Stents Design and their Translation into Clinical Practice”, *Research and Methodology*, vol.43,pp.89-100.
32. *Cardiovascular Physiology*, Page 3.
33. *Mechanical Engineering Reference Manual Ninth Edition*.
34. Klabunde, Richard (2005), “Cardiovascular Physiology concepts”, *Lippincott Williams & Wilkins*, pp.93-4.
35. Atherton.A and Bates.A, “Robust Optimization Of Cardiovascular Stents:A Comparison Of Methods,” *Journal Of Optical Engineering*,vol.00,pp.1-11,2003.
36. Bharat.M, Tom.B and Ghaus Malik, “Stent-within-a-Stent Technique for the treatment OF Dissecting Vertebral Artery Aneurysms,” *Am J Neuroradiol*, vol.24, pp.1814-1818, 2003.
37. Fernandez.SF, Tandar.A, Boden.WE, “Emerging medical treatment for angina pectoris,” *Expert opinion on emerging drugs*, vol.15, Issue.2, pp.283-98, 2010.
38. Isam.F, Rosaire.M, Richard.L, Joseph.R, Eric.L and Olivier.B, “Time-dependent 3D simulations of the Hemodynamics in Stented Coronary artery,” *Biomedical Materials*, Vol.2, 2007.

39. Kaazempur.M, Wada.S, Myers.G and Ethier.R, “Mass Transport and fluid flow in stenotic arteries:Axisymmetric and Asymmetric models,” International Journal Of Heat and Mass Transfer,Vol.48, pp.4510-4517, 2005.
40. Kajzer.W and Marcinaik.J, “Experimental and Numerical analysis of urological stents,” International Journal Of Material Science and Engineering, Vol.5, Iss.5, pp.297-300, 2007.
41. Lally.C, Dolan.F and Prendergast.J, “Cardiovascular Stent Design and Vessel Stresses:A finite Element Analysis,” Journal Of Biomechanics,Vol.38, pp.1574-1581, 2005.
42. Luis.A, JoseI.A, Iris.L and Luis.S, “Mechanics Biomaterials:Stents,” Applications Of Engineering Mechanics in Medicine,2004.
43. Masahiro.M, Akihiro.H, Shinzo.T, Kohsuje.T and Kazuo.S , “Experimental Study Of the Histocompatible Of covered Expandable Metallic Stents in the Trachea,” Chest Journal, Vol.114, pp.110-114, 1998.
44. Men-chi.H and T.S.Ravigururajan, “Biothermal Modeling of Post Cryoplasty Atherosclerosis in Restenotic Patients,” Cardiovascular Engineering, vol.7, pp.7-16, 2007.
45. Micheal.M, Nandini.D,Richard.S and James.M, “Stented Artery Flow Patterns and Their Effects on the Artery Wall,” Annual Review of Fluid Mechanics, vol.39, pp.357-382, 2007.
46. Niroomand.H, Tafazzoli.M and Farzan.G, “Flow Characteristics in Elastic Arteries Using a Fluid-Structure Interaction Model,” American Journal Of Applied Sciences,Vol.4, pp.516-524, 2007.
47. Pier.T, “Endoscopic Pancreatic Duct Stent Placement For Inflammatory Pancreatic Diseases,” World Journal Of Gastroenterology, vol.13, pp.5971-5978, 2007.
48. Pochrzast.M, Walke.W, Kaczmarek, “Biomechanical characterization of the balloon-expandable slotted tube stents,” Journal of Achievement’s in Material and Manufacturing Engineering, Vol.37, Issue.2, 2009.
49. Rupak.B, Surendra.D, Diwakar.R and Lloyd.B, “Developed pulsatile flow in deployed coronary stent,” Journal of biorheology, Vol.44, Iss.2, pp.99-102, 2007.
50. Schulz.C, Herrmann.A, Beilharz.C, Pasquantonio.J and Alt.E,“Coronary Stent symmetry and Vascular injury determine experimental stenosis,” Jouranl Of Heart, Vol.83, pp.462-467, 2000.

51. Sravan.K, Ramji.T, Arun.M and John.C, "Thermal Injury Prediction during Cryoplasty through in Vitro Characterization of Smooth Muscle Cell Biophysics and Viability," *Journal of Biomedical Engineering*, Vol.36, pp.86-101, 2008.
52. TA-Wei.D and Bing-Shiun-W, "Effects of Hematocrit Level on the Blood flow in the Corrugated Vessel due to the implantation of Intravascular stents," Vol.18, Issue.2, 2006.
53. Thomas.F, Mourad.L, Thomas.B.W, "Computational Fluid Dynamics: Hemodynamic changes in Abdominal Aortic Aneurysm After Stent-Graft Implantation," *Cardiovascular Intervent Radiol*, Vol.29, pp.613-623, 2006.